Project No.	ON-00454
Contract No.	450009661 and 450009663
AWI Project Manager	Bridget Peachey
Contractor Name	CSIRO and The University of Queensland
Prepared by	Dr Andrew Kotze and Professor David Fairlie
Publication Date	June 2020

New Chemicals for Sheep Blowfly Control

Published by Australian Wool Innovation Limited, Level 6, 68 Harrington Street, THE ROCKS, NSW, 2000

Executive Summary

Control of the sheep blowfly relies largely on the use of chemical insecticides applied as preventative treatments to protect against flystrike. However, recent reports of the emergence of resistance to the most commonly-used chemicals threaten the sustainability of the industry, and have highlighted the need for alternative drugs for flystrike control. The present project aimed to explore one avenue of this drug development process by examining the potential for blowfly control based on the use of inhibitors of a specific target in the blowfly. The target was a group of enzymes that play a vital role in cell development in most organisms, histone deacetylase enzymes (HDACs). In recent years there has been a great deal of interest in developing inhibitors of these enzymes in humans as possible treatments for cancers, inflammatory diseases, and parasitic diseases. The present project aimed to identify inhibitors of HDAC enzymes for use as insecticidal compounds for the control of the sheep blowfly.

Experimental HDAC inhibitors were synthesised, and their ability to kill blowfly larvae was measured using *in vitro* assays. We also measured the ability of the compounds to inhibit the blowfly HDAC enzymes. We undertook repeated rounds of compound synthesis and testing, using the results of each round to inform on structural changes to be made to compounds for the next round of synthesis. We also performed a comprehensive homology modelling study to generate likely structures of the blowfly HDAC enzymes. This then allowed us to model the fit of experimental drugs into the enzymes. The homology modelling also allowed us to study differences that exist between the structures of the enzymes in blowflies and mammals, with a view to exploring the potential for drug design of insect-specific inhibitors. Finally, to begin to translate our study from the lab to the field, we conducted a small scale larval-implant trial on sheep using several of our experimental compounds. We examined the ability of blowfly larvae to establish strikes on sheep that had been treated with the experimental drugs.

The most potent compounds identified in the study had very significant levels of activity against blowfly larvae *in vitro* and were also potent inhibitors of blowfly HDAC enzymes. The best of the compounds was within 4-fold as toxic to blowfly larvae as the commercial blowfly control chemical cyromazine (the active ingredient in Vetrazin, ProGuard, Lucifly and Cy-Guard) in our *in vitro* assays. Importantly, the most potent compounds showed an ability to inhibit the early larval life stages of the blowfly, with complete inhibition of larval growth within the first 24 hours at the highest concentrations tested. This speed of action of the compounds is an important aspect for their potential as insecticides as it is vital for a blowfly control chemical to prevent the larvae developing to a stage that can start to cause significant damage to the sheep.

We constructed *in-silico* homology models for each of the five blowfly HDAC proteins *Lc*HDAC1, 3, 4, 6 and 11, as identified in its genome. The various blowfly HDACs had between 44 -78% sequence identity with their respective human HDACs (1, 3, 4, 6, 11). We analysed the amino acid differences between the blowfly HDACs and their corresponding human HDACs near the binding site. We found the binding sites of three of the blowfly enzymes were very similar to human binding sites, with few differences. Hence, the design of inhibitors that are selective for these blowfly enzymes over their human counterparts will be challenging. On the other hand, for another of the blowfly enzymes (*Lc*HDAC6), we found significant sequence differences between the human and blowfly binding sites. Drug docking studies confirmed the presence of a number of differences near the binding site of the human and blowfly HDAC6 enzymes. These differences in residue size, charge and polarity may allow the design of new inhibitors that may prove to be more potent and selective towards blowfly HDACs.

Finally, we conducted a sheep trial in which experimental compounds were applied to implant sites on sheep, and the subsequent ability of blowfly larvae to establish infections at these sites was measured. We applied cyromazine (ProGuard) to some sites as a commercial insecticide treatment to compare to our experimental compounds. We tested three experimental inhibitors, chosen on the basis of potency against blowfly larvae *in vitro*, high microsomal metabolic stability, presence of structurally-distinct features, and low synthetic cost. Two of the three compounds killed all the larvae at the experimental sites. The level of drug required to kill all larvae was approximately 5-fold higher than the levels of cyromazine required to achieve the same outcome. This indicates that the experimental compounds were able to prevent blowfly larval growth at a concentration comparable to that for the commercial product cyromazine.

We investigated whether any of the experimental drugs were blowfly-specific inhibitors (that is, inhibitors of blowfly HDAC enzymes, but not of mammalian HDAC enzymes), but found no evidence for this. However, as mentioned above, the homology modelling work showed that a focus on the *Lc*HDAC6 enzyme offers potential for the discovery of such blowfly-specific inhibitors in the future. It is also clear that complete insect-specificity may not be required for blowfly control as the potency of the experimental compounds identified here means that they can likely be used at levels safe for topical application to mammals, as required for blowfly control in sheep.

This project has shown that HDAC inhibitors are potent inhibitors of blowfly larval growth and development *in vitro*, and has identified new potent compounds. We have shown that the most active compounds are also able to prevent the development of larvae at experimental implant sites on sheep. Further work to build on the outcomes of the present study to develop HDAC inhibitors as insecticides for blowfly control will require the project team engaging with animal health companies.

CONTENTS

1. Introduction/Hypothesis

Recent reports of resistance to cyromazine- and dicyclanil-based products for control of the sheep blowfly have highlighted the need to identify new insecticides for the control of this parasite. The present project aimed to address this issue by exploring a potential new chemical and structural class of insecticidal compounds for blowfly control. The new compounds sought here will have a completely different mechanism of action from current and known insecticides, in order to minimise and delay by many years the onset of drug resistance emerging to a new class of insecticides. The target we are examining is a group of enzymes known as histone deacetylases (HDACs) which have recently been identified in blowflies. The project aligns with current international efforts to develop inhibitors of human HDAC enzymes for various applications in medicine, including the control of parasitic diseases of humans. The project aims to provide evidence for this approach to blowfly control, including the identification of compounds with potent activity against blowfly larvae and the blowfly HDAC enzymes. Information gathered during the project will be used by the project team to engage with animal health companies to further develop a new insecticide class.

Hypothesis: targeting histone deacetylase enzymes can provide opportunities for the development of new insecticides for the control of the sheep blowfly.

2. Literature Review

The Australian sheep blowfly (*Lucilia cuprina)* is an important ecto-parasite that causes fly strike, which has significant health, welfare and economic impacts on the sheep industry in Australia. The female blowfly is attracted to the sheep by odours, particularly those associated with bacterial infections in damp fleece, and lays eggs. The developing larvae feed on the sheep, causing severe tissue damage, toxaemia, and can cause death. The consequent loss of livestock, costs of preventative and curative chemical treatments, and animal welfare issues, place significant economic burdens on livestock enterprises. An MLA-commissioned study in 2015 reported that the blowfly parasite costs the Australian sheep industry about $180M per annum (MLA 2015).

The control of this important parasite relies largely on the use of insecticides applied to the sheep as preventative treatments. However, over many years the blowfly has developed resistance to various classes of chemical insecticides used for its control, including organochlorines, organophosphates, the benzoyl-phenyl urea diflubenzuron, as well as the triazine cyromazine. Levot et al. (2012, 2014) reported low level resistance to dicyclanil in a laboratory strain derived from survivors of a field treatment with cyromazine. Sales et al (2020) has recently described blowfly field strains showing significant levels of resistance to dicyclanil. The resistance results in significantly reduced periods of protection from flystrike after application of various dicyclanil-based products.

Resistance to ivermectin has not yet been reported in the blowfly, however its use for many years against gastrointestinal worms of livestock has resulted in high levels of resistance (Kotze and Prichrad 2016), hence highlighting the likelihood of resistance emerging in blowflies in the future. Similarly, resistance to imidacloprid has not been reported in the sheep blowfly but has emerged in areas where the compound has been used for the control of other insects and arachnids (Bass et al., 2015). This history of the emergence of resistance in insects, including the blowfly, necessitates constant efforts to identify new insecticides, preferably with different target proteins and different mechanisms of action than the current insecticides.

Histone deacetylases (HDACs) are enzymes that are essential for the regulation of gene transcription in all organisms, but their structures are different in different organisms. The blocking of their action with drugs results in cell death. In recent years there has been a great deal of interest in developing inhibitors of these enzymes in humans as possible treatments for cancers and inflammatory diseases. Several HDAC inhibitors are currently in clinical use as chemotherapy treatments for humans. They have also been studied over recent years for their potential in chemotherapy for parasitic diseases of humans, including malaria, toxoplasmosis, trypanosomiasis, schistosomiasis and leishmaniasis (Andrews et al., 2012). These international efforts to develop HDAC inhibitors for control of human parasitic diseases are reviewed here:

i) Malaria
A number of laboratories have been active in recent years in identification of HDAC inhibitors that may be useful for malaria control. An important component of this work is aiming to identify parasite-specific compounds. The Institutions involved in this work include Griffith University and the University of Queensland (Australia), Liepzig, Dusseldorf and Tubingen Universities (Germany), the Pasteur Institute and CNRS (France), the University of California (USA), and the university of Rome (Italy).

Reports of inhibitors that are selective for the malaria parasite over mammalian cells:

- Mackwitz et al. (2019) and Diedrich et al. (2018) examined a series of peptoid-based compounds. They identified compounds with potent activity against blood-stage malaria parasites (IC_{50} < 10 nM), and with selectivity indices vs human cells of > 1000-fold. Both studies highlighted the fact that targeting the parasite's HDAC6 may be a better strategy than targeting HDAC1 as compounds inhibiting the former seem to show much less toxicity towards mammalian cells.
- Chua et al. (2017) found selectivity indices of up to 45-fold for several HDAC inhibitors in killing malaria parasites compared to their effects on mammalian cells.
- Bouchut et al (2019) reported on a compound that showed potent inhibition of the malaria parasite (IC_{50} 4 nM) and selectivity indices of 186- and 783-fold against two human cell lines.
- Stenzel et al (2017) identified 5 compounds as potent inhibitors of malaria parasites, with selectivity indices of > 100-fold compared to mammalian cells. The compound that had the most potent activity against the parasite showed a selectivity index of > 455-fold.
- Avels et al. (2017) identified a potent inhibitor of malaria with a selectivity index of 25-fold
- Ontoria et al. (2016) and Engel et al. (2015) identified a number of compounds with selectivity indices of > 50 and up to 46-fold, respectively.

ii) Schistosomiasis (an important human disease caused by parasitic flatworms called schistosomes)
A great deal of work is underway to identify inhibitors of HDAC8 from *Schistosoma mansoni*. The work is funded by the European Union, and involves various laboratories in Germany, France and Japan.

This group identified schistosome HDAC8 as the best HDAC enzyme to target for control of this parasite as this enzyme showed the greatest differences in amino acid sequence and structural features of the active site compared to its human equivalent (Marek et al 2013, 2015). Quite early in this work, the group identified a compound that showed selectivity for the schistosome HDAC8 over the human HDAC8 (4-fold selectivity), highlighting the potential to identify schistosome-specific inhibitors (Stolfa et al 2014). Other studies have generally found that compounds that inhibit schistosome HDAC8 do not show selectivity for the parasite enzyme over the human form, however there have been several exceptions to this:

- Bayer et al. (2018) described a compound with 5-fold selectivity for the schistosome HDAC8;
- Stenzel et al. (2017a) identified a compound with 1.8-fold selectivity for schistosome HDAC8.
- Heimburg et al (2016) identified 6 compounds with selectivity indices of 1.8 – 6.2 fold for schistosome HDAC8. They also noted that most of the compounds only show 'relatively low effect' on mammalian cells.

Another feature of this HDAC8 work is that the most important selectivity may not be for human HDAC8 vs parasite HDAC8, but rather for HDAC8s in general vs other HDAC enzymes in general; that is, it may be best to look for compounds that may inhibit both parasite and mammalian HDAC8, but do not inhibit other mammalian HDACs. This strategy may be preferred as it has been reported that inhibition of human HDAC8 is not nearly as detrimental to human cells as is the inhibition of other human HDACs. Therefore, compounds that inhibit the parasite HDAC8 do not necessarily need to be inactive against the human HDAC8 as long as they show little activity against the other human HDACs. Hence, a number of the schistosome studies mentioned above have also focused on compounds that inhibit HDAC8 (in the parasite and or humans) but do not affect other human HDACs. They have reported on a number of compounds that fit this desirable pattern.

iii) Trypanosomes (parasites responsible for sleeping sickness, caused by *Trypanosoma brucei*, and leishmaniasis (a set of trypanosomal diseases caused by various species of *Leishmania*).

Trypanosoma brucei:
Two studies have shown that some HDAC inhibitors are active against *Trypanosoma brucei in vitro* (Engel et al 2015, and Carrilo et al 2015), thereby highlighting them as drug targets, however, the limited number of compounds tested to date do not show any parasite selectivity. Engel et al. (2015) reported that the HDAC inhibitor romidepsin showed potent activity against the parasite, with an IC_{50} of 35nM, however it did not show any selectivity for the parasite over mammalian cells.

Leishmania donovani:
Patil et al. (2010) and Guerrant et al. (2010) reported that several HDAC inhibitors were active against *Leishmania donovani*, however, the selectivity indices were all < 1.

iv) Crytosporidium (parasites that cause gastrointestinal illness (cryptosporidiosis))
Guo et al. (2018) showed that the HDAC inhibitor vorinostat showed potent activity against crytosporidium *in vitro*, as well as showing a selectivity index of 11.4-fold. They also showed that repeated treatments of mice over 6 days resulted in > 90 % reduction in parasite oocyte production, with no harmful effects on the mice.

3. Project Objectives

1. Use homology modelling to create three-dimensional structures for all the blowfly HDAC enzymes and perform *in silico* analysis of these structures in complex with putative small molecule ligands from an extensive database of millions of chemical structures. The aim is to identify known or new compounds predicted to be most likely to interact with these enzymes and thereby identify structural requirements for potent insecticidal compounds.

2. Synthesise novel chemicals as prospective inhibitors of blowfly recombinant HDAC enzymes. Test compounds as inhibitors of blowfly HDAC enzymes and for their ability to kill blowfly larvae.

3. Perform repeated rounds of structure-activity assessments and chemical modifications on our experimental compounds in order to optimise inhibition of blowfly HDACs, killing of blowfly larvae, insect specificity and to derive the most practical compounds for development into a useful, stable, safe and cost-effective new insecticide for the intended market.

4. Industry engagement: compile information on chemical structures of insect-specific HDAC inhibitors with potent insecticidal activity, taking into account many factors that influence most appropriate compound selection for further development, in order to build a marketable portfolio of data that can attract investment from an animal health company. Such a partner will be sought for ultimate development and commercialisation of a novel class of insecticides for future blowfly control.

4. Success in Achieving Objectives

1. Homology modelling: we successfully completed a comprehensive modelling study with the blowfly HDACs. This indicated that Class I blowfly HDACs are very similar to their mammalian counterparts, and hence blowfly-specific drugs targeting these enzymes may be difficult to develop. On the other hand, Class II HDACs were significantly different from their mammalian counterparts, opening up the possibility of blowfly drugs that do not target mammalian HDACs.

2. Synthesis and testing of novel chemicals: We completed 10 rounds of compound synthesis, amounting to over 200 compounds synthesised. Each compound was tested against blowfly larvae and two recombinant blowfly HDAC enzymes. Most compounds were also tested against a recombinant human HDAC enzyme.

3. Perform repeated rounds of structure-activity assessments: the results of testing of each compound batch was used to inform on the structural changes to make to the compounds of the subsequent batch. This process was repeated for 10 batches of compounds. This process was successful in identifying several compounds with potent insecticidal activity. The best compound had an IC_{50} against blowfly larvae within 4-fold of that shown by cyromazine.

We were not successful in identifying any insect-specific inhibitors. The activity of our experimental compounds against the blowfly HDAC1 enzyme was correlated with their activity against the human HDAC1 enzyme. Hence, insecticides of this type are likely to also inhibit the human version of the blowfly target enzyme, if they were to be administered to humans via injection. However, the method of use is proposed to be topical administration to mammals (sheep) and it is unlikely that this class of prospective insecticide would ever be absorbed by humans, nor would it likely be topically toxic to sheep. Further work is needed to confirm this.

4. Industry engagement: The information we have compiled on i) compound structural features conferring insecticidal activity, ii) homology modelling compound design predictions, and iii) the successful demonstration of insecticidal activity in a sheep trial, will all be important components of future engagement with animal health companies. We have not yet developed a formal partnership with an industry partner**.**

5. Methodology

5.1 Recombinant enzymes

We worked with the Protein Expression Facility (PEF) at the University of Queensland to produce recombinant versions of three of the blowfly HDAC enzymes. We had worked with them in our earlier AWI-funded project (ON-00110) to produce small amounts of two of these enzymes. However, these had been quite unstable to storage at -80^{o}C, and hence were not suitable for use in a series of enzyme assays conducted over a period of time as was required for the present project. Hence, we aimed to generate larger amounts of the recombinant enzymes, and develop methods to ensure that the enzymes were stable in storage at -80^{o}C. We chose to produce three separate blowfly HDAC enzymes: blowfly HDAC1 (as a representative of Class I HDAC enzymes), blowfly HDAC 6 (Class II), and blowfly HDAC11 (Class IV).

The PEF performed a series of enzyme expression trials in order to optimise the conditions for production of the three blowfly enzymes. This involved experiments in which various expression and enzyme purification conditions would be utilised at the PEF, and then CSIRO would measure the activity of the different enzyme solutions in order to identify the optimum method. This would then inform on the set of conditions to examine in greater depth in the next series of experiments.

5.2 Experimental compound synthesis

Experimental HDAC inhibitors were synthesised in the laboratory of Professor Fairlie. All reagents were purchased from Sigma-Aldrich, Combi-Blocks Inc. or Chem-Impex International Inc. Most compounds were chemically synthesized by conventional solution phase approaches. Microwave-driven chemical reactions were performed using a Biotage Robot Eight 2.3 build 6250. Compounds were purified from reaction mixtures by preparative reversed phase HPLC separations, which were performed on a Phenomenex Luna C18 10 µm, 250 Å~ 21.2 mm column. Standard conditions were used for elution of all compounds with 100% A to 100% B linear gradient over 15 min followed by a further 10 min at 100% B at a flow rate of 20 mL/min. Solvent A was H2O + 0.1% TFA and solvent B was 90% MeCN, 10% H2O + 0.1% TFA. Compounds were detected by UV light and pure fractions were lyophilized to white powders.

All final compounds were analyzed by NMR spectroscopy (1H and 13C NMR) and mass spectrometry (UPLC-MS and HRMS) and purity was determined to be >95%. 1H and 13C NMR spectra were recorded on a Bruker Avance III HD 600 spectrometer at 298 K in the deuterated solvents indicated. 1H NMR spectra in DMSO-d6 were referenced to the residual 1H signal at 2.50 ppm, CDCl3 solutions were referenced to internal TMS. 13C NMR spectra were referenced to the solvent peak DMSO-d6 at 39.51 ppm. The exact concentration of the compounds in solution was determined by quantitative NMR integration 'PULCON' experiments. Analytical UPLC-MS was performed on a Shimadzu Nexera equipped with a 2020 ESI-MS and diode array detectors. The column was a Zorbax Eclipse plus C18, 1.8µm, 95Å, 2.1 x 100 mm monitored at three different wavelengths (λ 214, 230 and 254 nm). Standard elution conditions were used for all compounds, linear gradient 100% A –100% B over 5 min followed by a further 1 min at 100% B, flow rate 0.5 mL/min. Solvent A was water + 0.1% formic acid and B was 90% MeCN 10% water + 0.1% formic acid. Preparative rpHPLC was conducted on a Phenomenex Luna column C18, 21.5 x 250 mm at flow rate 20 mL/min using same solvents as analytical except TFA 0.1 % was used in place of formic acid.

5.3 Assays with blowfly larvae and recombinant enzymes

5.3.1 Bioassays with blowfly larvae

Each of the experimental compounds was examined in assays with blowfly larvae using methods described by Kotze et al (2015). These assays measure the effects of the compounds on two aspects of the development of blowfly larvae:

i. The effect on the weight gain of 1st instar larvae over the first 24 hours of their development (this indicates potency and speed of action of the compound).
ii. The effect on the rate of pupation of larvae at the end of the larval growth phase of the life cycle (this indicates whether any effects seen in the early life stages in i) are maintained across the entire period of larval development).

The effects of the compounds on larval growth were measured over a range of compound concentrations between 200 and 0.32 µg/assay. Each concentration was examined in replicate assays. Groups of 55 freshly-hatched larvae were added to assay pots containing sheep serum-soaked cotton wool that had previously been treated with a compound. After 24 hrs, five larvae were removed, weighed as a group and discarded. The remaining larvae continued to develop in the assay pot over the next week. Pots were then placed into larger containers to allow fully-developed larvae to migrate out of the original pot and into sand in the outer container, and pupate. Numbers of pupae were counted 7 days later. Larval weights (at the 24 hr time point) and numbers of pupae were expressed as percentages of the measurements recorded from control (no drug) assays. Non-linear regression was then performed using GraphPad software in order to generate dose-response curves, and IC_{50} values.

Compound IC_{50}s represented the concentration of compound required to reduce the weight gain or pupation rate to 50 % of that measured in control assays.

5.3.2 Assays with recombinant HDAC enzymes

The ability of the compounds to inhibit the activity of the recombinant blowfly HDAC enzymes was assessed using a standard HDAC enzyme substrate (assay kits purchased from Sigma Aldrich Chemical Co.). The effects of each compound on the activity of the two recombinant enzymes (*Lc*HDAC1 and *Lc*HDAC6) were measured across a series of compound concentrations. The highest drug concentration tested was 10,000 nM. Drug concentrations were then decreased until the drug did not inhibit the enzyme activity (activity equivalent to control assays in the absence of drug). This allowed for dose-response curves and IC_{50} values to be generated using GraphPad software. Compound IC_{50}s represented the concentration of compound required to reduce the enzyme activity to 50 % of that measured in control (no drug) assays.

In addition, most of the compounds were also examined in enzyme assays in Prof. Fairlie's lab for their effect in inhibiting the activity of a recombinant human HDAC1 enzyme (*Hs*HDAC1). IC_{50} values for this inhibition were calculated as described above.

5.3.3 Microsomal stability assays

A small number of compounds were examined in Prof. Fairlie's lab to determine their susceptibility to metabolic breakdown by the enzymes present in microsomes prepared from rat liver tissue. Microsomes are known to contain large amounts of various enzymes that are able to degrade xenobiotics, including insecticides. The most important and predominant group of enzymes are the cytochrome P450 enzymes. This liver microsomal assay was conducted in order to compare the metabolic stability among the small set of selected experimental compounds.

Microsomes were prepared by centrifugation of a rat liver homogenate, with the microsomes recovered as the pellet from a 100,000 x*g* 60 minute spin. Drugs were added to microsome solutions, and samples taken at various times. Undegraded drug was recovered from these samples and quantified using the UPLC-MS techniques (see 'compound synthesis', section 5.2). The rate of degradation of the drug over time was used to calculate its half-life, equivalent to the time taken for the amount of drug to be reduced to half its level at the beginning of the incubation period.

5.4 Homology modelling

Protein sequences of *Lc*HDACs 1, 3, 4, 6 and 11 were downloaded from Uniprot (www.uniprot.org) in fasta format. A BLAST sequence search of the RCSB-Protein Data Bank (PDB) (www.rcsb.org) determined structural homologs of each lcHDAC. Crystal structure templates were identified for each LcHDAC and downloaded from the PDB. LcHDAC sequences and crystal structures were read into the Chimera software package (www.rbvi.ucsf.edu/chimera) and aligned using a BLOSUM62 matrix including a 30% secondary structure score. The program Modeller (salilab.org/modeller) was used to generate 30 all atom homology models that included appropriate binding site hetero and water atoms from crystal templates. Final lcHDACs 1, 3, 4, 6 and 11 models were chosen by their lowest energy DOPE score and best GA341 score; final structural quality was assessed with Molprobity (molprobity.biochem.duke.edu). Docking of inhibitors into lcHDACs homology models was conducted using Glide software (Glide, Schrödinger, LLC, New York, NY, 2020) in extra precision mode. Docked inhibitors were further optimized in the binding site using Prime MMGBSA (Prime, Schrödinger, LLC, New York, NY, 2020).

5.5 Sheep implant experiment

The ability of three of the experimental HDAC inhibitors to inhibit the growth of blowfly larvae on sheep was examined using a larval implant technique originally described by Eisemann et al (1989) for assessing the ability of blowfly larvae to establish infections on sheep in order to determine the immune status of the sheep. The three drugs were chosen after consideration of their potency against the larvae in *in vitro* assays, their high microsomal metabolic stability, and with a view to select three structurally-distinct compounds. The 3 drugs were named as: BR67c, JT86b and LD42.

All animal procedures were approved by the CSIRO Armidale Animal Ethics Committee, approval number 19/04. Six wether sheep (castrated males), aged approximately 15 months, were selected for the experiment.

Day 1: an area from the shoulder to the end of the rib cage and over the backbone was clipped with electric shears. Oster clippers were then used to remove the wool as close to the skin as possible at four sites (100 mm in diameter) on each sheep (two per side). Foam rings were then attached to the skin sites using silicone sealant (SikaSeal®, Sika Australia Pty Ltd.) (Figure 1). Sheep coats were placed on each animal.

Figure 1: Rings in place on a sheep

Day 2: Each ring was checked to ensure it was secured properly. A disposable razor was used to gently abrade a circular area of skin (approximately 10 mm diameter) in the centre of the skin area enclosed by the foam ring.

Drug solution was applied slowly to each ring site (Figure 2). The solutions applied to each ring are described in Table 1, with the locations of each treatment shown in Figure 3. Each sheep had one control site and 3 drug treatment sites. With a total of 24 sites available (4 x 6), three of the drug treatments were selected for use in the 'spare' rings, giving duplicate sites for these three drug treatments (see Table 1).

Figure 2: Adding drug to a ring site

Table 1: Stock drug solutions, and amounts of each drug applied to ring sites on sheep

Compound	Stock solution	Volume applied to ring[a]	Amount of drug applied to ring (mg)	Single (S) or duplicate (D) assays
BR67c	50 mg/mL in ethanol	i) 1 mL stock ii) 0.5 mL of x5 dilution ii) 0.5 mL of x50 dilution iii) 0.5 mL x 500 dilution	i) 50 ii) 5 iii) 0.5 iv) 0.05	D S S S
JT86	25 mg/ml in ethanol	i) 1 mL stock ii) 0.5 mL x 2.5 dilution iii) 0.5 mL x 25 dilution iv) 0.5 mL x 250 dilution	i) 25 ii) 5 iii) 0.5 iv) 0.05	S D D S
LD42	2.5 mg/mL in ethanol	i) 1 mL stock ii) 0.5 mL x2.5 dilution iii) 0.5 mL of x25 dilution	i) 2.5 ii) 0.5 iii) 0.05	S S S
cyromazine (ProGuard)	Commercial product, 60 mg/mL	i) 0.5 mL of x 30 dilution in water ii) 0.5mL of x300 dilution iii) 0.5 mL of x3000 dilution iv) 0.5 mL of x30,000 dilution	i) 1 ii) 0.1 iii) 0.01 iv) 0.001	S S S S

[a.] dilution was in ethanol, except for cyromazine diluted in water

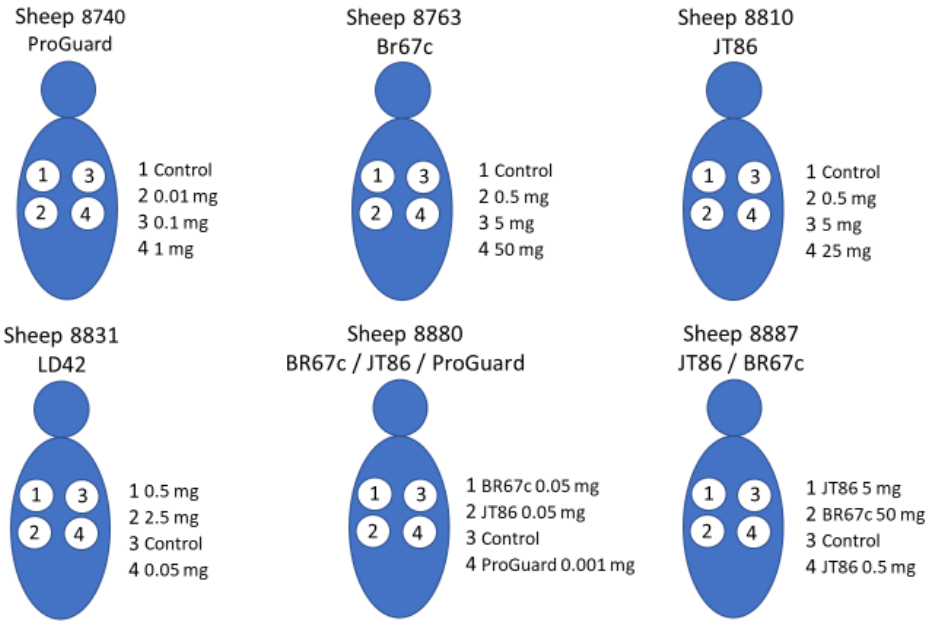

Figure 3: Drug and control treatment sites on the 6 sheep.

After approximately 5 hours, the placement of freshly-hatched blowfly larvae onto the ring sites commenced. Groups of 200 were collected in a volume of approximately 0.5 mL water, and then slowly deposited on a disc of blotting paper. The paper was immediately inverted and placed into the centre of the ring site. Discs of moist absorbent cloth were then placed on top, and the site was sealed with a mesh cloth (Figure 4).

Figure 4: Assembled drug sites on a sheep.

Day 3, 24 hours after larvae had been added to sites: Each site was inspected, and note was taken of any dead larva on the paper disc or lowest cloth, the presence of live larvae at the site, and their approximate size.

Day 4, approximately 44 – 48 hours after larvae had been added to sites: The sites were inspected and any live larvae were collected into pre-weighed containers. The wound site was searched thoroughly and all larvae were collected. The containers were then re-weighed, and frozen. The foam rings and silicone sealant were carefully removed from each site. The sites were treated with Alamycin Aerosol Topical Spray, followed by Extinosad™ Eliminator. The larvae collected from each site were later defrosted and counted.

6. Results

6.1 Recombinant enzymes

6.1.1 Blowfly HDAC1 enzyme (*Lc*HDAC1)

We performed a series of experiments looking at the optimal conditions to produce the blowfly HDAC1 enzyme in a form that was stable to storage at -80°C. The PEF then used this set of conditions to produce a large amount of the recombinant enzyme for us in February 2018 (Figure 5, left panel). The enzyme was active in our assay, with initial experiments showing that several experimental HDAC inhibitors showed dose-dependent inhibition of its activity (Figure 6).

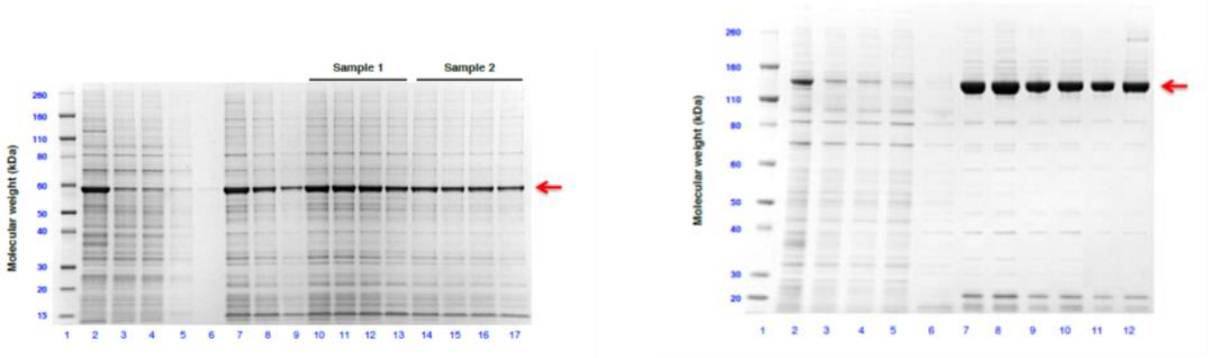

Figure 5: SDS-PAGE gels of blowfly HDAC enzymes at various stages of production.

Left panel: blowfly HDAC 1 enzyme; right panel: blowfly HDAC6 enzyme. Lanes on the left hand side of the gels represent early stages of the purification; lanes on the right hand side of the gels represent later, more pure, stages of the purifications. Arrows at the right side show the positions of the blowfly enzymes.

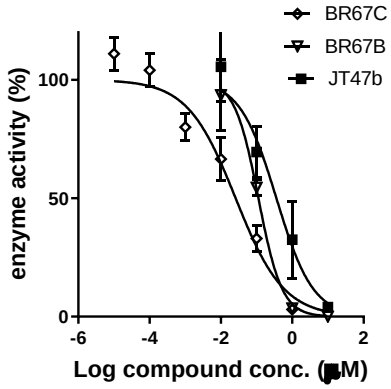

Figure 6: Effect of three experimental HDAC inhibitors on the activity of the recombinant blowfly HDAC1 enzyme.

6.1.2 Blowfly HDAC 6 enzyme (*Lc*HDAC6).

We also worked with PEF on stability issues with this enzyme and were able to develop a method of producing enzyme that was stable to storage at -80°C. The PEF produced a large amount of the enzyme for us in May 2018 (Figure 5, right panel).

6.1.3 Blowfly HDAC 11 enzyme

We performed a number of experiments with the PEF, aiming to express and purify this enzyme, however, we could only produce very small amounts. The PEF looked at several different expression systems, however, they were unable to produce sufficient amounts of this enzyme for us to use in assays with the experimental inhibitors. We therefore decided not to pursue this enzyme any further for the present project.

6.1.4 Assays measuring inhibition of recombinant HDAC enzymes by experimental compounds.

The results of assays measuring the inhibition of the recombinant HDAC enzymes by the experimental compounds generated in this study are described below, in section 6.2, alongside the results of assays with blowfly larvae.

6.2 Chemical synthesis, and activities against blowfly larvae and blowfly enzymes

6.2.1 Experimental compounds

We examined a series of batches of chemicals over the course of the project as follows (batches named according to date transferred from the Fairlie lab to the Kotze lab):

2018:	Feb	19 compounds
	April	11
	June	24
	August	22
	September	43
	November	20
	December	21
2019:	April	10
	May	32
	August	4
		Total = 206

Most of the compounds were in the form of both a powder and a solution in the solvent DMSO. The former were used in larval bioassays, while the latter were used for enzyme assays with the recombinant blowfly HDAC enzymes. In a small number of cases, the experimental drugs could only be supplied in solution in DMSO, and hence it was not possible to assess the compounds in the larval bioassay (blowfly larvae are particularly susceptible to DMSO and hence it is not possible to use it as a solvent for bioassay experiments).

Figure 7 shows some commercially-available HDAC inhibitors with activity against sheep blowfly larvae (from Bagnall et al., 2017), illustrating some of the structural features of the experimental compounds from the present study.

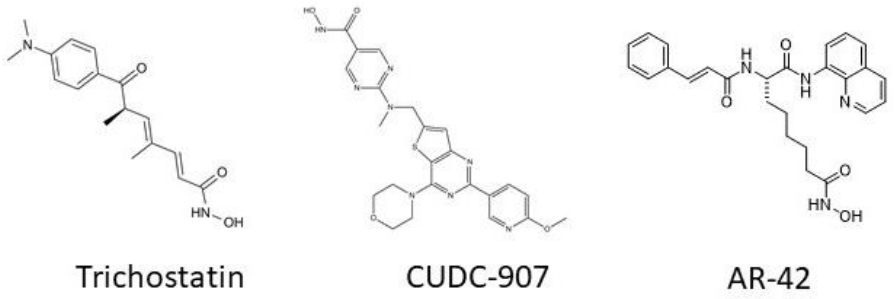

Figure 7. Structures of commercially-available HDAC inhibitors with activity against sheep blowfly larvae *in vitro* (from Bagnall et al., 2017).

6.2.2 Bioassays with blowfly larvae

IC_{50} values for the effects on larval weight gain (over the first 24 hrs of the larval life-stage) and pupation were calculated for each experimental compound. Compounds that did not inhibit weight gain or pupation to less than 50 % of controls at the highest concentration tested (200 µg/assay) are reported as having IC_{50} values of > 200.
It is important for any experimental compound to show activity with both measurements. That is, to show rapid effects to prevent the early growth of the larvae, and then to also ensure that this effect is maintained across the entire larval growth phase so that the larvae do not recover from an initial set-back to resume normal development. The range of values for the weight gain IC_{50} across the compounds in each batch across the entire study is shown in Figure 8, panel A.

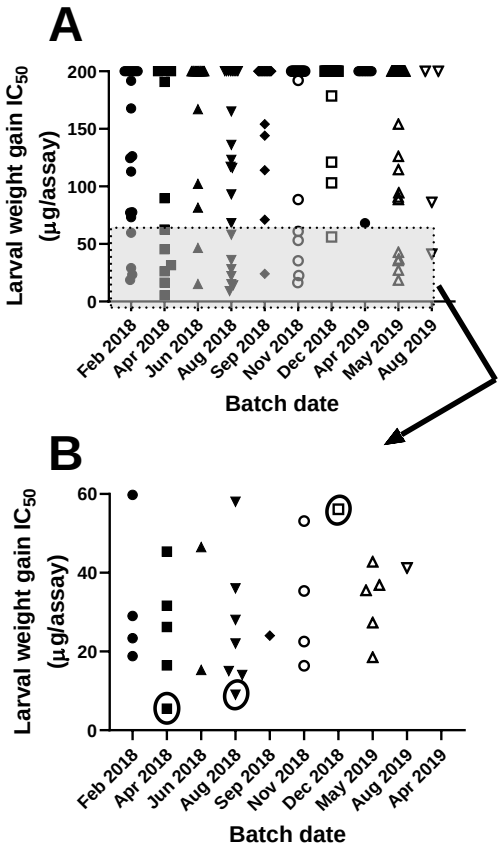

Figure 8: Larval weight gain IC_{50} values for chemicals in each compound batch; **A:** all data; **B**: focus on compounds with weight gain IC_{50} < 60 µg / assay. The three compounds used later in sheep experiment are circled.

Within each chemical batch shown in Figure 8, there were a number of compounds that were not active against the larvae (data points across the top of the Figure). These compounds did not reduce the weight gain to less than 50 % of controls at the highest concentration tested (200µg). The most potent compounds (highlighted at the lower part of panel A) are shown more clearly in panel B.

The three compounds used in the sheep experiment are circled in Figure 8B. The IC_{50} values for these three compounds were: 5.4, 9 and 56 µg/ assay. The IC_{50} values for the two most potent of these compounds (BR67c and JT86b) compare favourably with the IC_{50} of 1.29 for the commercial blowfly insecticide cyromazine in our assays (as shown for BR67c in Figure 9). The experimental compound BR67C had a weight gain IC_{50} within 4-fold of the value for cyromazine. The IC_{50} for the compound was however 45-fold greater than that for the widely-used blowfly insecticide dicyclanil.

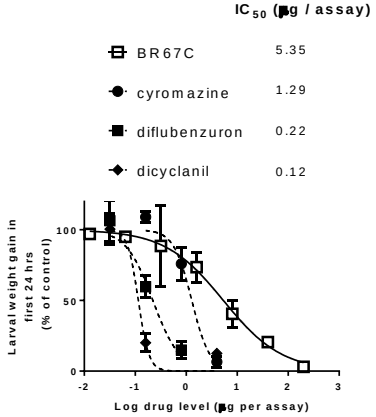

Figure 9: Effects of commercial blowfly insecticides and BR67C on development of blowfly larvae *in vitro.*

As described in the methods section, the effect of each experimental compound on blowfly larvae was described with IC_{50}s for larval weight gain over the first 24 hrs of the larval life stage, as well as effects on pupation. Figure 10 shows a comparison of the two measurements for each compound.

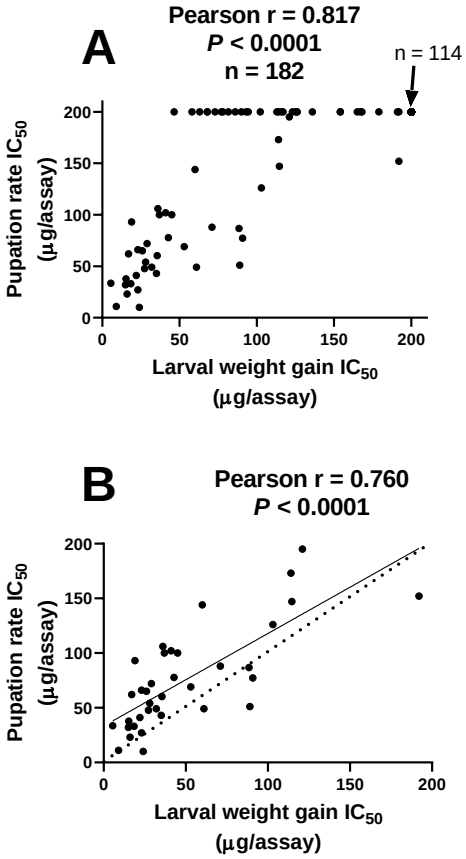

Figure 10: Comparison of the effects of each experimental compound on larval weight gain and pupation *in vitro;* **A**: all compounds; **B**: just the most potent compounds, solid line = regression, dotted line = 1:1 ratio of the two IC_{50}s.

Figure 10, panel A, indicates that quite a number of compounds were effective inhibitors of the early stages of larval growth (X-axis, weight gain IC_{50} < 200), however a number of these were not effective in inhibiting pupation (pupation IC_{50} shown as 200 µg, points across the top of the Figure). Hence, for these compounds, early effects on larval growth were not maintained in the later stages of growth, and many larvae were able to continue to develop as normal to pupate. Such a temporal effect on larval growth would be unsuitable for blowfly control.

However, it is also clear from panel A of the Figure that many compounds inhibited both larval weight gain and pupation. This is examined more closely in panel B which only shows the compounds with IC_{50} values less than 200 µg (that is, only the most potent compounds). The two IC_{50} values were significantly correlated (P < 0.001). The dotted line shows a 1: 1 relationship between the weight gain and pupation measurements. The data would be expected to follow this line if the IC_{50} for the two measurements were equivalent. The solid line shows the actual relationship between them. It is apparent that the actual line is an approximation of the line expected if the IC_{50}s were equivalent. Hence, for these most potent of the experimental compounds, the effects on larval weight gain were maintained over subsequent days as the larvae developed further and pupated. That is, there was minimal recovery from the early insecticidal effects, as would be desirable in any blowfly control chemical.

Note that we did not perform any experiments to optimise compound structures for absorption into blowflies or for blowfly pharmacokinetics or pharmacodynamics.

6.2.3 Relationships between larval growth inhibition and HDAC enzyme activity inhibition

i) Blowfly HDAC1 enzyme (*Lc*HDAC1)

The ability to inhibit the activities of the two blowfly HDAC enzymes (*Lc*HDAC1 and *Lc*HDAC6) was measured for each of the experimental compounds. Compounds that did not inhibit activity of the HDAC enzymes to less than 50 % of controls at the highest concentration tested (10,000 nM) are reported as having IC_{50} values of > 10,000.

The results for *Lc*HDAC1 are shown in Figure 11.

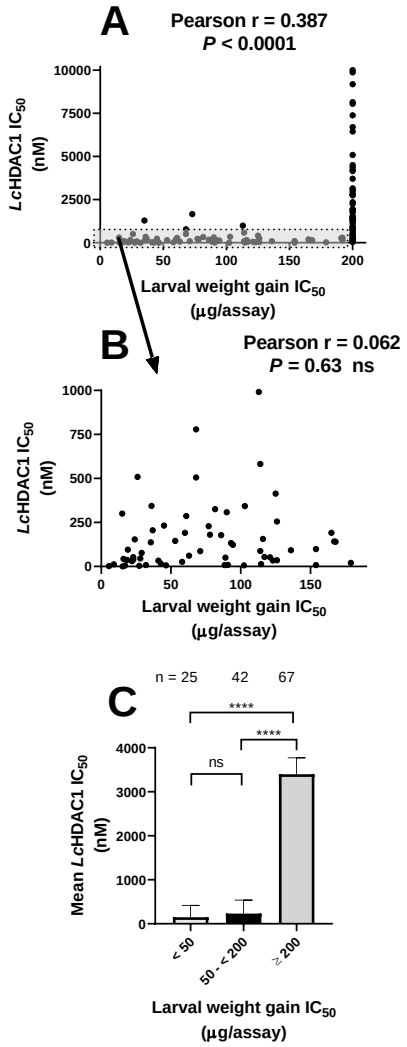

Figure 11: Possible relationship between the inhibition of larval weight gain and inhibition of *Lc*HDAC1 activity by each experimental compounds; **A**: full data set; **B**: focus on only the compounds that inhibited larval growth; **C**: the whole data set grouped into three broad bands.

Points to note from Figure 11:

- the compounds that had no effect on larval growth (weight gain IC_{50} given as 200 µg in panel A) showed a range of effects on the activity of the enzyme (IC_{50}s varying from 0.6 to >10,000 nM). The two variables were significantly correlated ($P < 0.0001$).
- for the compounds that did show an effect on larval growth (panel B), there was no correlation between their effects on larval development and their effects on *Lc*HDAC1 enzyme activity ($P = 0.63$). That is, for this group of compounds, their ability to inhibit the blowfly enzyme was not directly related to their ability to inhibit larval growth. Therefore, their effect on enzyme activity could not be used to predict the relative potency of these compounds against the larvae.
- however, despite this inability to use enzyme data to predict larval activity at potency levels of below 200 ug/assay, it is clear from panel C that the effects of experimental compounds on *Lc*HDAC1 enzyme activity may be a useful means to identify compounds that have either no activity against larvae or have activity with

an IC_{50} of < 200. That is, the assay could be useful as a broad initial screen to identify compounds likely to be insecticidal among a collection of potential HDAC inhibitors, without being able to define relative potency on a finer scale.

ii) Blowfly HDAC6 enzyme (*Lc*HDAC6)

The results for *Lc*HDAC6 are shown in Figure 12.

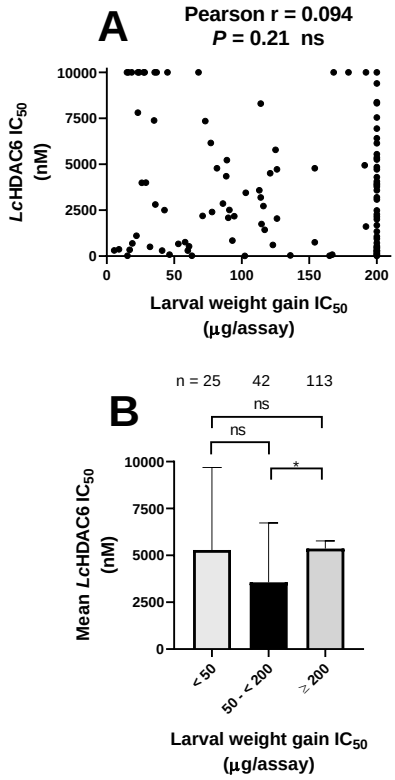

Figure 12: Possible relationship between the inhibition of larval weight gain and inhibition of *Lc*HDAC6 activity by each experimental compounds; **A**: full data set; **B**: the whole data set grouped into three broad bands.

Points to note from Figure 12:

- as described above for *Lc*HDAC1, the compounds that had no effect on larval growth (weight gain IC_{50} given as 200 µg in panel A) showed a range of effects on the activity of the *Lc*HDAC6 enzyme (IC_{50}s varying from 2.3 to >10,000 nM). In addition, a number of compounds showed no effects on the enzyme (points across the top edge of the Figure) alongside potent inhibition of larval development.
- there was no correlation between effects on larval growth and effects on *Lc*HDAC6 enzyme activity (*P* = 0.21).
- in contrast to *Lc*HDAC1 described above, the grouping of larval activity into broad bands did not indicate any relationship between larval activity and *Lc*HDAC6 inhibition (compare Figure 11 panel C with Figure 12 panel B).
- while the activity of the experimental compounds against *Lc*HDAC6 was of interest to the project (as described in the homology modelling section of this report), it is important to note that the compounds were designed with a view to inhibiting HDAC1 enzymes rather than HDAC6 enzymes. Hence, it is not unexpected that their insecticidal activity was more closely related to their activity against *Lc*HDAC1. Most of the compounds would have been expected to act more strongly against the blowfly HDAC1 enzyme rather than the HDAC6 enzyme when fed to the larvae in the larval bioassay experiments.

We also examined a batch of compounds that are known to be selective towards inhibition of mammalian HDAC6 enzymes over HDAC1 (the April 2019 compound batch). Nine of the ten compounds were not active in the blowfly larval assay (weight gain IC_{50}s> 200 µg). The remaining compound only showed a low level of activity, with an IC_{50} of

68 µg. This result may be due to the differences highlighted in the homology modelling section of this report between the human and blowfly HDAC6 enzymes.

iii) Human HDAC1 enzyme (*Hs*HDAC1)

Many of the experimental compounds were also examined in assays with recombinant human HDAC1 enzyme (*Hs*HDAC1). Their ability to inhibit this enzyme was compared to their effects on the blowfly HDAC1 enzyme (Figure 13).

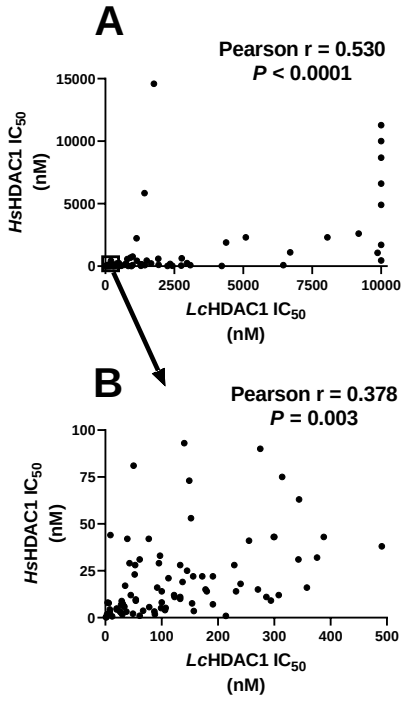

Figure 13: Possible relationship between the inhibition blowfly HDAC1 (*Lc*HDAC1) and human HDAC1 (*Hs*HDAC1) by the experimental compounds; **A**: full data set; **B**: focus on just the most potent inhibitors.

The effects on the two enzymes were significantly correlated ($P < 0.001$). Panel B of the Figure shows the relationship for just the compounds that were most potent against the two enzymes (*Lc*HDAC1 IC_{50} < 500 nM, and *Hs*HDAC1 IC_{50} < 100 nM). Again, the inhibitory effects of the compounds on the two enzymes were significantly correlated ($P = 0.003$).

This observed correlation between the ability of the compounds to inhibit the blowfly and human HDAC1 enzymes is not surprising given the similarities between the two enzyme catalytic sites in terms of amino acid sequences and homology modelling (as described in the modelling section of this report). The modelling work indicated that such similarity between the active sites of the two enzymes will make it unlikely that we can design any inhibitors to target the blowfly HDAC1 without also inhibiting the human HDAC1 (although there is no intention of administering such compounds to humans or systemically to mammals). Figure 13 reinforces that point. We do not consider this to be a problem, as the intention is to apply compounds topically to sheep.

6.2.4 Microsomal metabolism

A small number of compounds were examined in assays with microsomes prepared from rat liver. This assay measures the metabolic stability of the compounds in the presence of the detoxification enzymes (predominantly cytochrome P450s) present in the microsomal preparation. While normally used to determine how metabolically stable a compound may be when administered to a human patient, we were interested in how stable the compounds may be when exposed to the detoxification enzymes that would be present in the blowfly, particularly the cytochrome P450s that are known also to be produced in blowfly microsomes.

Our earlier comparison of blowfly larval weight gain IC_{50} values and HDAC1 inhibition IC_{50} values had shown a poor correlation between the two variables when looking at just the most potent compounds (Figure 11, panel B). A possible explanation for this was that such an analysis did not account for the activity of detoxification enzymes in

the blowfly, which may allow more readily detoxify some compounds compared to others. It is likely that the experimental drugs show such differences in their susceptibility to breakdown by microsomal enzymes. Hence, we performed a limited series of assays to measure stability of some of the experimental compounds in the presence of microsomal enzymes (using mammalian microsomes as a proxy for blowfly microsomes). The data is shown in Figure 14 panel B, however an explanation of the analysis is first given in panel A.

Points to note from Figure 14, panel A:
- X-axis = the ratio between the larva weight IC_{50} of a compound, over the effect of the compound on the blowfly HDAC1 enzyme
    - if this ratio is high, the larval IC_{50} is high compared to the enzyme inhibition IC_{50}, therefore the compound is less potent against the larvae than may be expected given its enzyme IC_{50}
    - if this ratio is low, then the two IC_{50} are more similar, then the compounds potency (weight gain IC_{50}) is more in agreement with its enzyme IC_{50}.
- Y-axis = compound half-life in the presence of the microsomes
    - a stable compound has a long half-life
    - an unstable compound (ie, easily metabolised by microsomal enzymes) has a short half-life

The dashed line on panel A shows the expected relationship between the two variables if microsomal enzymes contributed to less than expected potency in the experimental compounds in assays with blowfly larvae (the relationship is shown here as being linear for illustrative purposes only).

Our limited data set with experimental drugs (n= 9) is shown in Figure 14, panel B. The outcome of linear regression analysis is shown as a solid line. Although the relationship was not significant ($P > 0.05$) there was a trend for the variables to show the expected relationship shown in panel A, that is, decreasing compound half-life as weight gain IC_{50} increased relative to LcHDAC1 inhibition IC_{50}.

This suggests that compound stability may at least partly explain the lack of correlation observed earlier between potency against larvae and potency in inhibiting the LcHDAC1 enzyme (Figure 11, panel B). That is, compounds that were very potent inhibitors of the LcHDAC1 enzyme, but were not potent inhibitors of larval weight gain, may have lacked the larval activity due to their susceptibility to breakdown by detoxification enzymes present in the larvae. This analysis emphasises the need to consider metabolic stability of the experimental HDAC inhibitors in blowflies, alongside their ability to inhibit LcHDAC1, as the two factors will influence their ability to inhibit larval growth.

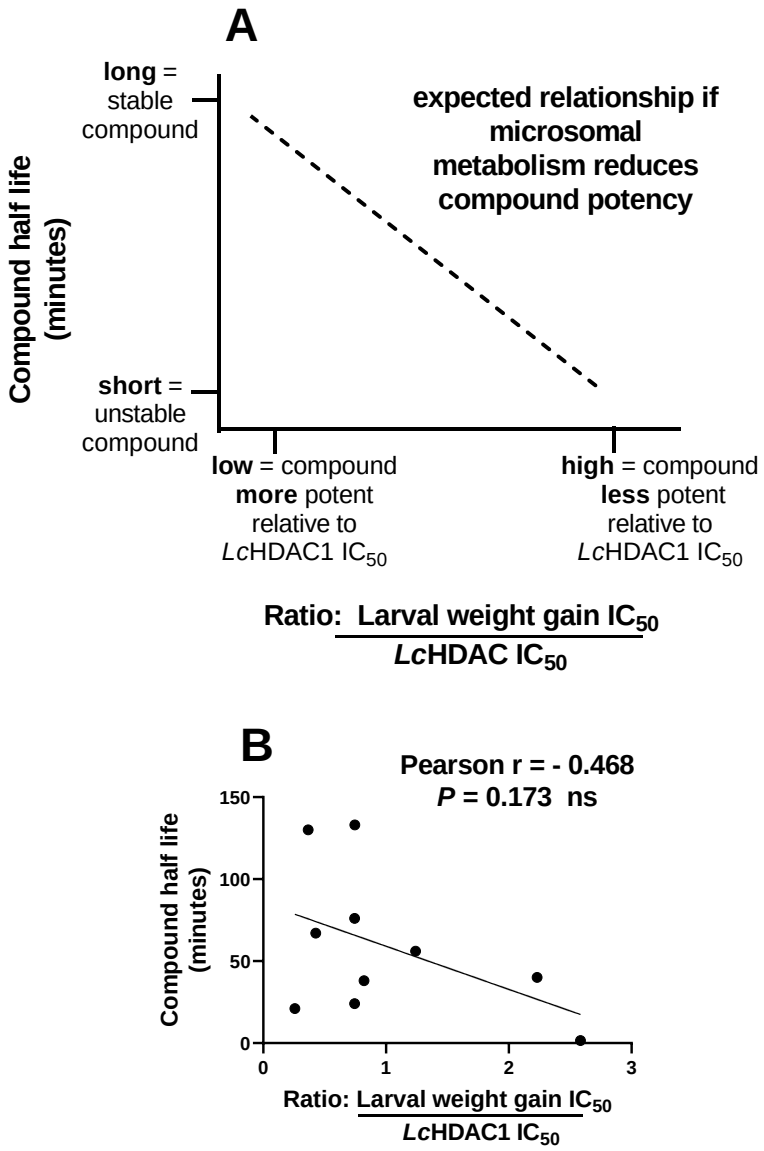

Figure 14: Relationship between microsomal metabolism and potency in inhibiting larval weight gain for a limited set of experimental compounds; **A**: illustration of the nature of the analysis, see text for details; **B**: data set.

6.3 Homology modelling

We initially focused our molecular modelling analysis on a previously identified human and blowfly HDAC inhibitor AR-42. AR-42 has two diastereomeric forms (*R*- and *S*-) which were docked into a well-established crystal structure of a human HDAC homolog (Figure 15). The resulting docked poses of (*R*-) and (*S*-)AR-42 gave consensus docking scores of 77 and 108 respectively. The consensus scores and docked poses were consistent with the (*S*-) diastereomer being five times more potent than the (*R*-) as a HDAC inhibitor. Having established we could successfully dock AR42 into the HDLP crystal structure revealing important interactions between AR42 and HDLP. We decided to construct homology models of lcHDACs to enhance our structure-based discovery of new inhibitors.

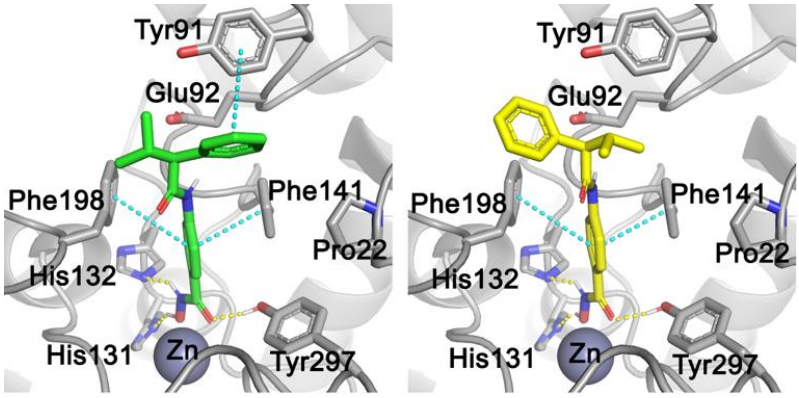

Figure 15. Molecular docking of *S*- (left) and *R*- (right) isomers of AR42 into a HDLP-TSA complex (PDB : 1c3r.pdb). Each isomer makes favourable interactions with the Zn^{2+} atom and H-bonds (yellow dotted lines) to His131, His132 and Tyr297. Stereochemistry accounted for a five-fold difference in the inhibitory potency against human HDAC1, due to favourable hydrophobic and/or *pi-pi* interactions (cyan dotted lines) between the phenyl ring and Phe198 and Phe200 for both isomers and additionally to Tyr91 for the *S*- isomer.

Sequence analysis of the catalytic domains of lcHDAC1, 3, 4, 6 and 11 show 78%, 68%, 59%, 44% and 55% sequence identity with the respective human HDACs. A sequence alignment of blowfly and human HDACs, including 3D structural information, shows fully conserved amino acids highlighted with coloured backgrounds in Figure 16. Highlighted amino acids are not only conserved in the sequences but are structurally conserved where there is 3D information available. LcHDAC1 Zn^{2+} chelating amino acids D176, H178 and D264 are fully conserved in all lcHDACs. Residues important for lysine-acetate hydrolysis near the active site H138, H139 are also fully conserved. Residues G147, F148, C149, F203 and P204 that are close to, or form part of, the hydrophobic tunnels are also highly conserved.

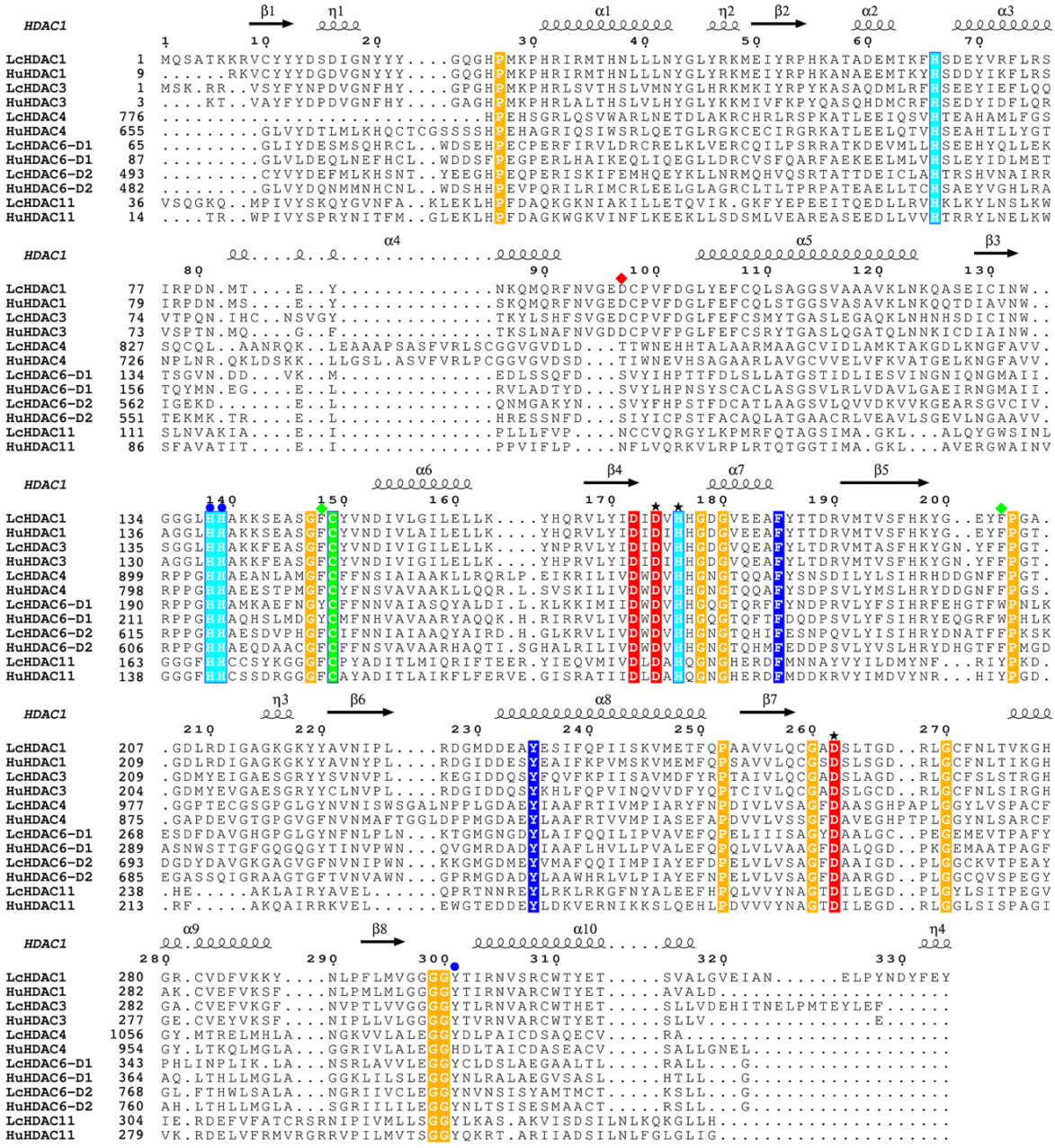

Figure 16. T-Coffee sequence alignment of lcHDACs and hsHDACs including 3D crystal structure sequence information. Secondary structure from hsHDAC1 crystal structure (5ICN.pdb) is displayed above; α = alpha-helix, η = 3_{10}-helix, β = beta-strand. Strictly conserved residues shown with highlighted with solid colour background, black stars above sequences are HDAC1 catalytic Zn^{2+} chelating residues, blue spots are residues implicated in lysine-acetate hydrolysis, green diamonds represent binding site hydrophobic tunnel residues and red diamonds are H-bond donor/acceptor residues at entrance to the hydrophobic tunnel important for ligand binding.

Currently, there are no crystal structures of lcHDACs, however crystal structures of HDACs from human and other species are available. In the absence of crystal structures, 3D homology models of lcHDACs derived from sequence alignments with human HDACs for which there are crystal structures, can provide valuable structural information on ligand binding sites in lcHDAC proteins. We have now constructed homology models for the catalytic domains of lcHDAC1, 3, 4, 6 and 11 to determine amino acid differences between blowfly and human HDACs near the catalytic Zn binding site. Protein sequences corresponding to lcHDAC1, 3, 4, 6 and 11 were downloaded from Uniprot (www.uniprot.org). Blowfly lcHDAC 6 like human and other HDAC6 enzymes contain two catalytic domains lcHDAC6-D1 and lcHDAC6-D2. LcHDAC sequences were then individually submitted to a BLAST search of the RCSB-Protein Data Bank (PDB) (www.rcsb.org) to determine structural homologs of lcHDACs. Structures suitable to act as templates for homology modelling were selected based on their sequence identity (% Identity, higher is better) towards the lcHDAC sequences and their resolution in angstroms (Resolution Å, lower is better). Generally, if the

template crystal structure has sequence identity of ≥35 % with the sequence being modelled then a reliable model can be constructed. Similarly, crystal structure quality is important for production of a reliable homology model, this is reflected in the resolution (in Å) of the structure - a resolution of ~1 Å is high quality whereas resolution of >3.5 Å is low quality. We found lcHDAC1, 3, 4, 6-D1, 6-D2 all had crystal structure templates with sequence identity ≥45 % and resolutions <2.1 Å. Currently there are no reported crystal structures of HDAC11, and lcHDAC11 has only 26 % sequence identity with human HDAC1 and HDAC2 crystal structures. Crystal structures of homologous proteins were identified and downloaded for use in homology modelling, Table 2.

Table 2. Crystal structure homologues of lcHDACs for homology modelling.

Lucilia cuprina sequence	Homologue sequence of PDB*	PDB entry	% Identity	Resolution Å
lcHDAC 1	hsHDAC1	5ICN	83	3.3
	hsHDAC2	4LXY	83	1.5
	hsHDAC1	4LXZ	83	1.8
lcHDAC 3	hsHDAC3	4A69	73	2.0
	hsHDAC2	4LXZ	62	1.8
	hsHDAC2	4LY1	62	1.5
lcHDAC 4	hsHDAC4	2VQM	59	1.8
	hsHDAC4	2VQO	59	2.1
lcHDAC 6 D1	drHDAC6 D1	5G0G	45	1.5
	drHDAC6 D2	5G0H	45	1.6
lcHDAC 6 D2	drHDAC6 D2	5EEK	54	1.6
	drHDAC6 D2	5EEI	54	1.3
lcHDAC 11	hsHDAC1	5ICN	26	3.3
	hsHDAC2	4LXZ	26	1.8

* crystal structure pdb sequences are either human (hs) or zebrafish danio rerio (dr).

The homology model of lcHDAC1 was created from sequence (Uniprot entry: A0A0L0C7T4) that was aligned to structural homologues belonging to human HDAC1 (5ICN.pdb) and HDAC2 (4LXZ.pdb, 4LY1.pdb). LcHDAC1 and crystal homologue sequences were aligned in Chimera (www.cgl.ucsf.edu/chimera) using a BLOSUM62 matrix including a 30% secondary structure score. Modeller (salilab.org/modeller) was then used to create homology structural models based on the alignment of lcHDAC1 and crystal structure homologues. 30 homology models including ligand SAHA and water atoms were created using a slow refinement procedure. Model quality was accessed using DOPE and GA341 methods in Modeller with the final lcHDAC1 model being chosen based on the best reported DOPE and GA341 scores, Table 3. Molprobity was also used to independently assess the models and give a score representative of an expected crystal resolution, Table 3. Homology models for lcHDAC3, 4, 6-D1, 6-D2 and 11 were successfully created in a similar way based on structural analogues found in the PDB and listed in Table 2. Model quality of lcHDAC1, 3, 4, 6-D1, 6-D2 and 11 was assessed to be suitable for structure-based drug design, results are shown in Table 3.

Table 3. LcHDAC homology model quality assessment.

Homology Model	DOPE[a]	GA341[b]	MolProbity[c]
lcHDAC1	-1.88	1	2.38
lcHDAC3	-1.70	1	3.13
lcHDAC4	-0.69	1	3.39
lcHDAC6-D1	-1.69	1	3.39
lcHDAC6-D2	-1.69	1	2.83
lcHDAC11	-0.45	1	3.53

a) A normalized discrete optimized protein energy (DOPE) potential, more negative values indicating better model quality b) GA341 model quality scale from 0 to 1, score >0.6 represents an accurate model. c) model quality score that represents expected crystallographic resolution.

The structures of lcHDAC1, 3, 4, 6-D1, 6-D2 and 11 constructed showed typical HDAC protein folds characterized by a single α/β domain, including eight β sheets sandwiched between up to eight α helices.(Dowling, Di Costanzo et al.

2008) Surrounding the core α/β domain are smaller α helices and short β sheets elements (Figure 17, light orange) linked by flexible loops. Surface secondary structure elements and protein loops provide a unique pattern of residues close to the binding site that enable selective ligand binding or selective protein-protein interactions during regulation of lcHDAC activity.

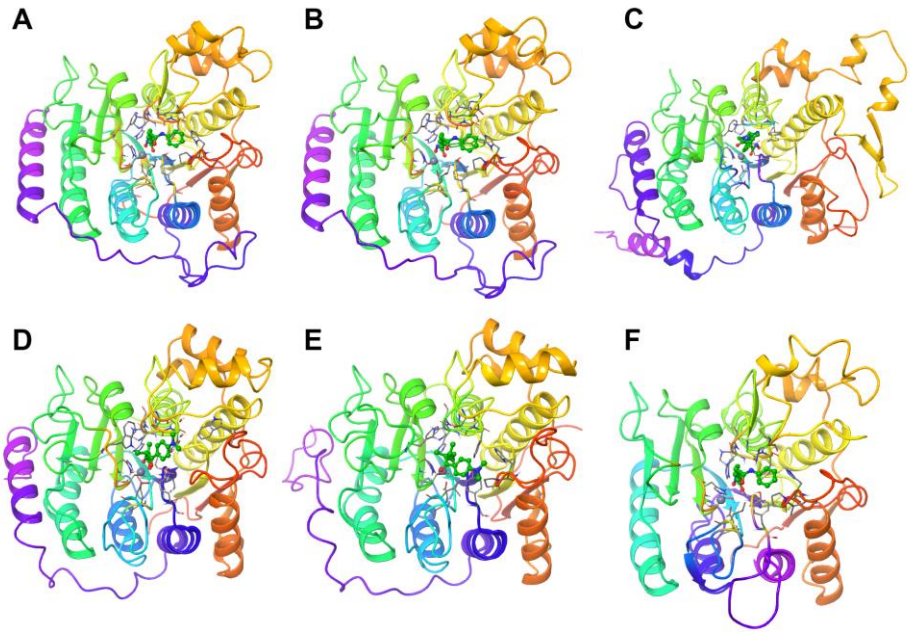

Figure 17. Homology models of lcHDAC1, 3, 4, 6-D1, 6-D2 and 11 represented as a rainbow cartoons A to F respectively. Shown is the active site Zn atom (grey sphere), active site ligand from template crystal structure (green ball and sticks) and residues within 4 Å of ligand (grey thin sticks).

We compared the binding sties of the Class I human and blowfly HDACs 1 and 3. Active site residues within 8 Å of modelled inhibitor SAHA bound to lcHDAC1 are nearly identical to hsHDAC1, Figure 18 (left). All active site surface exposed residues are identical, the only differences between blowfly and human HDAC1 are inaccessible to ligands and are buried below the surface at positions lc-V175 to hs-I177 and lc-A261 to hs-S263. Identical residues near the active site surface will make it challenging to design new lcHDAC1 specific inhibitors.

Similarly comparing of residues within 8 Å of the homology model of lcHDAC3 ligand with the corresponding hsHDAC3 crystal structure revealed 2 differences in sequence identity. The first difference lc-E97 to hs-D is both surface and ligand accessible whereas the second lc-V176 to hs-I is not. Differences between and human and blowfly HDAC3 near the active site result in a small contraction of the space available at the entrance of the binding pocket, Figure 18 (right).

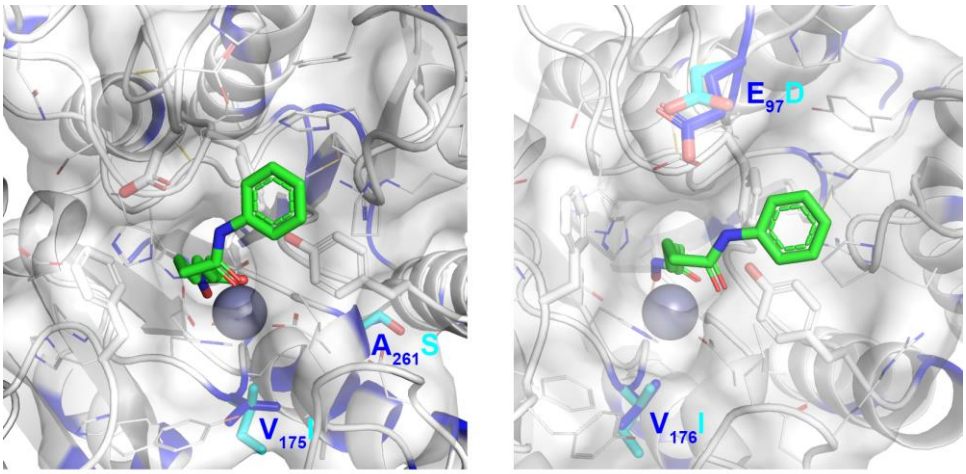

Figure 18. Homology models of lcHDAC1 (left) and lcHDAC3 (right) represented as a ribbon with human identical residues white and differing residues blue. A white solvent accessible surface is shown on residues within 8 Å of the

crystal ligands (green sticks) with non-identical residues shown as sticks (blowfly blue, human cyan,) and active site hydrophobic phenylaniline residues in white sticks.

Class I HDACs are also known to contain a narrow 14 Å internal channel that runs from the Zn atom and exits near Y24, H28 of hsHDAC1. This internal channel is thought to allow the release of acetate form the active site following deacetylation of histone lysine residues. LcHDAC1 and 3 also contain the internal channel with only minor differences observed between human and blowfly. LcHDAC1 G134 is smaller and less hydrophobic than hsHDAC1 A136, this might allow for the design of slightly large inhibitors in this region. Similarly, a single difference is for the internal channel for lsHDAC3 was found, lsHDAC3 S35 is larger and more polar than hsHDAC3 A130.

The homology model of Class IIa lcHDAC4 shows active site residues within 8 Å of the modelled are nearly identical to hsHDAC4. Only one surface residue lcHDAC4-Tyr1078 is different to hsHDAC4-His332. Interestingly, human HDAC4 structures containing a His332Tyr mutation and bound hydroxamate inhibitor have the tyrosine sidechain rotated towards the hydroxamate ligand in a similar pose to Class I HDAC structures as shown by the black arrow in Figure 19. The internal acetate release channel that is observed in blowfly and human Class I HDACs is closed off in Class II HDACs by a conserved R-E salt bridge from loop 1 to loop 3. These residues are conserved in the Class II lcHDAC 4 and 6 respectively and effectively close off the internal channel.

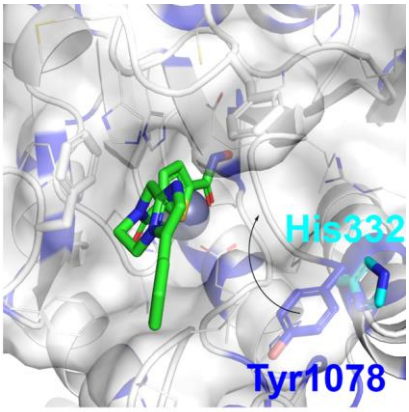

Figure 19. Homology model of lcHDAC4 represented as a ribbon with human identical residues white and differing residues blue. A white solvent accessible surface is shown on residues within 8 Å of the crystal ligands (green sticks) with non-identical residues shown as sticks (blowfly blue, human cyan,) and active site hydrophobic phenylaniline residues in white sticks.

Homology models of lcHDAC6-D1 (Domain1) and lcHDAC6-D2 (Domain2) were constructed on crystal structures of zebrafish drHDAC6 domains 1 and 2, which have higher sequence identity to lcHDAC6. Comparing the binding site of lcHDAC6-D1 with the human equivalent structures reveals five residues that are significantly different and accessible to the binding site, Figure 20 (left). The first is lsHDAC6-D1-E82 to hsHDAC6-D1-S, this introduces a negative charge in place of a small polar group. The neighbouring modification of lc-H83 to hs-F provides a polar aromatic group in place of a neutral hydrophobic group. A small polar group lc-S148 replaces the negatively charged hs-D sidechain. Polar aliphatic group lc-N265 replaces the larger aromatic polar sidechain of hs-H and finally lc-E332 to hu-K introduces a negatively charged group in place of the positively charged human lysine group. Analysis of the lcHDAC6-D2 binding site reveals five differences, the first is polar aromatic lc-Y507 relative to polar aromatic hu-W, Figure 20. On the same loop is a small constriction in binding site surface with the slightly larger negatively charged lc-E508 relative to hu-D. This is followed by an opening of the active site by inclusion of the smaller lc-G510 relative to the polar aromatic hu-H. The remaining two differences are on the opposite side of the ligand binding site with a small neutral polar group lc-N576 in place of hu-D a negatively charged group. The last difference is the positively charged group lc-K690 constricts the binding site relative to the smaller hydrophobic hu-M group. The acetate release channel that is present in Class I HDACS is again not present in lcHDAC6-D1 or -D2 due to the conserved R-E salt bridge from loop 1 to loop 3.

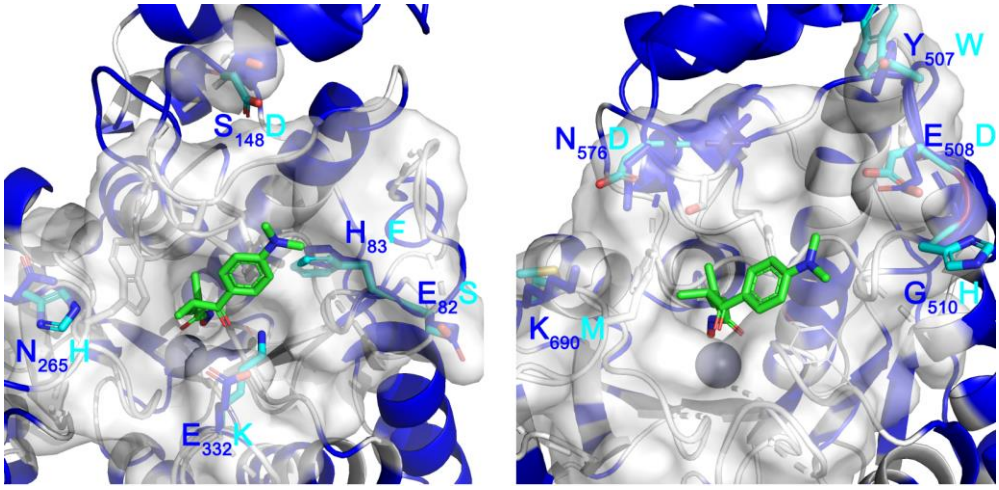

Figure 20. Homology models of lcHDAC6-D1 (left) and lcHDAC6-D2 (right) represented as a ribbon with human identical residues white and differing residues blue. A white solvent accessible surface is shown on residues within 8 Å of the crystal ligands (green sticks) with non-identical residues shown as sticks (blowfly blue, human cyan,) and active site tunnel residues in white sticks.

The final homology model to be completed was that of the Class IV lc-HDAC11, presented in Figure 17 (F). Currently there are no HDAC11 crystal structures from any source, there are also no structures with > 40% sequence similarity to lsHDAC11. Therefore, the homology model of LcHDAC11 was constructed on hs-HDAC1 and 2 structures 4BKX.pdb and 4LXZ.pdb respectively. Unfortunately, sequence similarity between lcHDAC11 and these structures is low at 26%. Producing a homology model with such a low level of sequence similarity means that while the constructed model is structurally sound; there are likely to be many problems with the size, shape and nature of the loop residues surrounding the binding site. A binding site analysis of lsHDAC11 was not undertaken as it would produce unreliable results.

Docking HDAC inhibitors was undertaken with the purpose of determining potential interactions between the inhibitors and lcHDACs. Docking focused on the homology models of lcHDAC1 and lcHDAC6-D2. This was done as many commercial HDAC inhibitors are active against Class I and II HDACs of which lcHDAC1 and 6 are representative. The second catalytic domain D2 of hsHDAC6 has broad substrate acetyllysine deacetylse activity while the first domain D1 is limited to specific substrates bearing C-terminal acetyllysine residues. We therefore focused our docking efforts the second domain of lsHDAC6-D2.

Initially, we investigated possible binding modes of AR-42 in lsHDAC1 active site (Figure 21 left). Ligand docking indicated that AR-42 (grey) had its terminal phenyl ring in a similar pose to that occupied by the phenyl ring from SAHA (Vorinostat). This pose is nearly identical to that observed in our earlier docking of AR-42 into HDLP, Figure A. The putative role of the chiral isopropyl group of AR-42 was investigated by comparing the docked poses of AR-42 (Figure 21, centre) with that of AR-42 with the isopropyl group removed (Figure 21, right). The docking results suggested that the presence of the isopropyl group may serve as a structural scaffold for directing the phenyl ring up towards a hydrophobic environment enclosing Phe155. These docking simulations guided new inhibitor designs to target lsHDAC1 and in particular to design inhibitors capable of H-bonding to the conserved lsHDAC1-D97 residue located at the entrance to the binding site, Figure 21 (left) and Figure 22.

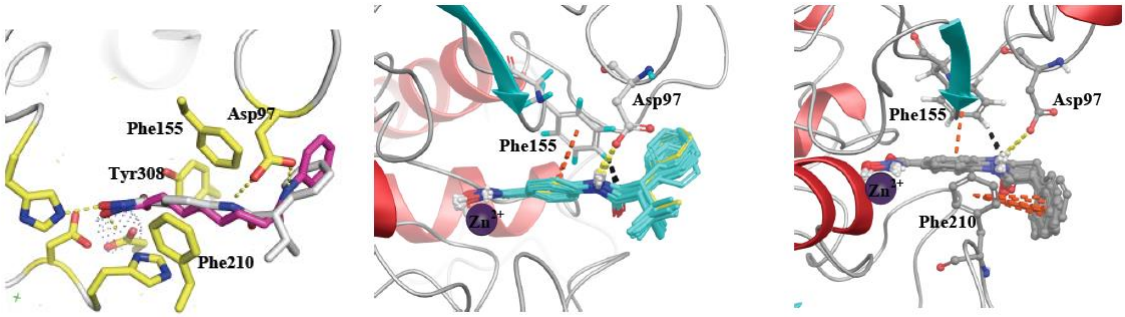

Figure 21. Molecular docking of AR-42 into blowfly lcHDAC1 structure. (left) Docked poses of AR-42 (grey) and SAHA (magenta) showing hydroxamic acid coordination to Zn^{2+} ion (dotted sphere), pi-stacking with Phe155, Phe210 and H-bond to distinct oxygens of lcHDAC1D97 (yellow lines). (Middle) 10 top scoring poses of AR42 with phenyl capping group projects towards Phe155; (Right) 10 top scoring poses AR42 analogue with isopropyl group removed, phenyl capping group projects towards Phe210.

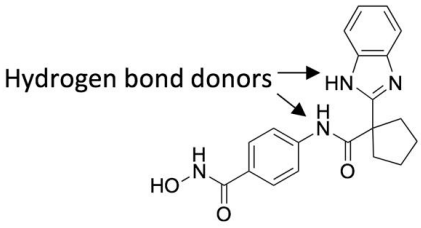

Figure 22. Designed putative inhibitor featuring NH hydrogen bond donors (indicated by arrows) designed to H-bond to lsHDAC1 D97.

Based on the initial AR-42 docking experiments a series of new ligands were designed to target conserved lsHDAC1 D97 residue by introducing H-bonding donor atoms into the structure of the inhibitor, as indicated Figure 22. Several of these newly designed inhibitors were successfully synthesised and found to be potent enzyme inhibitors of lcHDAC1 e.g. S2_E010, JT4-1-TFA, JT43, S2E17, JT9142_47a and JT9142-91-TFA.

Further lcHDAC1 docking experiments were undertaken with selected commercially available HDAC inhibitors Figure 23. Structures of the ligands were download from PubChem (pubchem.ncbi.nlm.nih.gov) and prepared for docking with the hydroxamic acid groups deprotonated to a metal ion binding form. Ligands were docked into lcHDAC1 and 6 respectively using the program Glide (Schrödinger Release 2019-2: Glide, Schrödinger, LLC, New York, NY, 2020) in extra precision XP mode and then optimized with Prime MMGBSA (Schrödinger Release 2019-2: Prime, Schrödinger, LLC, New York, NY, 2020).

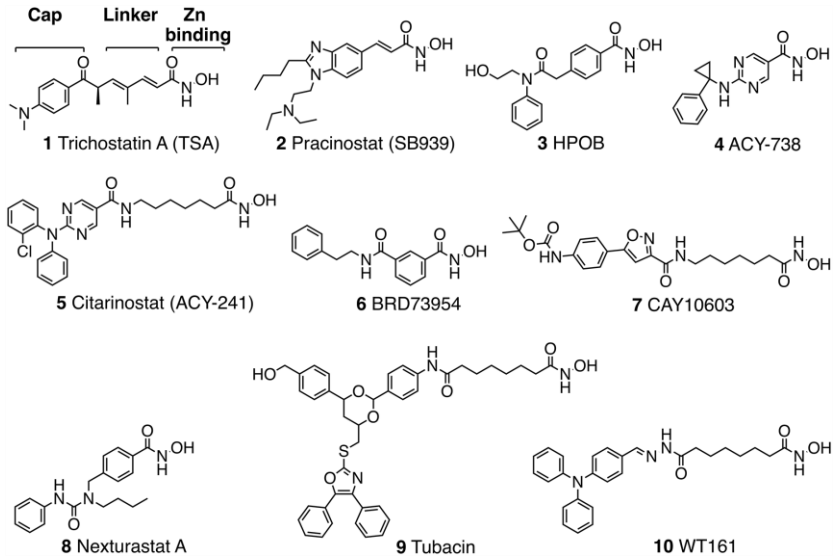

Figure 23. Selected commercially available HDAC inhibitors with Zn^{2+} binding, linker and cap regions shown on Trichostatin A.

All inhibitor hydroxamate groups bound the Zn^{2+} atom in a bidentate fashion with the carbonyl oxygen accepting a H-bond from lsHDAC1-Y301 and hydroxamate hydroxide O^- accepting a H-bond from lsHDAC1-H138, Figure 24. This bidentate interaction is observed in crystal structures of hydroxamic acid HDAC inhibitors. Inhibitor linking group regions were situated between LsHDAC1 F148 and F203 in the tunnel to the surface, Figure 24 (a). Inhibitors ACY-738, BRD73954, Trichostatin A, HPOB, Nexturastat A and CAY10603 have molecular weights (MW) < 450 and are smaller relative to the remaining inhibitors. Their capping groups were found to dock in the surface pockets near to the entrance to the zinc binding tunnel, Figure 24 (a). Capping groups of the larger inhibitors MW > 450 docked in extended conformations reaching further out onto the active site surface of lcHDAC1 sitting between surface between loops 1 and 2 or above loop 4, Figure 24 (b). Inhibitors Pracinostat SB939, HOPB, Nexturastat A (Figure 24, c, d, and e respectively), Tubacin, and ACY-241 docked in poses that allowed their H-bond donating groups to form a H-bond to lcHDAC1-D97 on loop 2 at the entrance of the Zn^{2+} binding site. The human homologous residue hs-D99 is required for HDAC deacetylase activity.

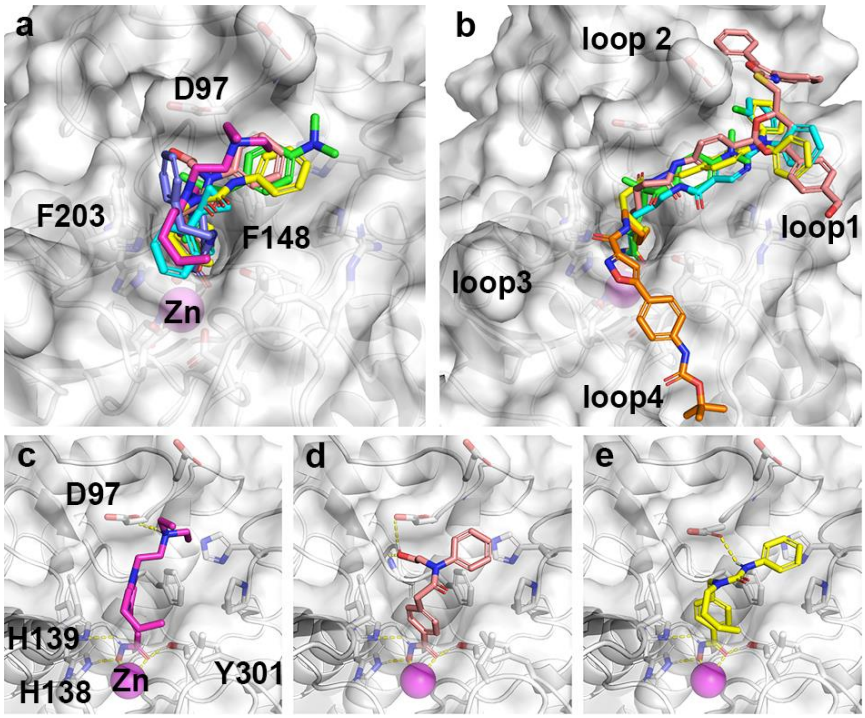

Figure 24. Prime MMGBSA optimised Glide XP poses of inhibitors in the lcHDAC1 binding site. LcHDAC1 as white ribbon with binding site residue sidechains shown as sticks (carbon, oxygen, nitrogen and hydrogen colored white, red, blue and white respectively) and Zn^{2+} atom as magenta sphere. a) Inhibitors MW < 450; b) Inhibitors MW > 450. Lower panel shows ligands; c) Pracinostat SB939, magenta sticks; d) HOPB, pink sticks; e) Nexturastat A, yellow sticks making polar interactions to active site Zn^{2+} atom and H-bonds to conserved residues D97, H138, H139 and Y301.

In human HDAC6 it is thought that the second catalytic domain D2 is responsible for deacetylase activity, with reported human HDAC6 inhibitors acting at this site. Initially the lcHDAC6-D2 homology model was used to dock HDAC inhibitors Bavarostat, and Nexturastat A and in-house inhibitors JT86B and JT19018-4. All the inhibitors were successfully docked in poses that satisfied the requirements of inhibitor binding. The hydroxamate groups were bound to the Zn^{2+} atom with the linking groups positioned in the hydrophobic tunnel and head groups siting at the entrance to the binding site. Bavarostat is a human HDAC inhibitor that shows 16000-fold selective inhibition of hsHDAC6 (IC50 60 nM) over hsHDAC1 (IC50 > 1000 uM) and has recently been co-crystallised with zebrafish drHDAC6-D2 (6VDO.pdb). Docking of Bavarostat into the lcHDAC6-D2 homology model showed good agreement (green sticks, Figure 25 panel a) with the corresponding co-crystalized drHDAC6-D2 conformation (white sticks, Figure 25 panel a), the main difference was the docked orientation of the meta-fluorine substituent away from the hydrophobic tunnel, whereas the crystal ligand placed the fluorine atom between the hydrophobic phenyl groups in the binding site tunnel. In a similar fashion inhibitors JT86B and JT19018-4 adopted similar poses (Figure 25 panels b and c).

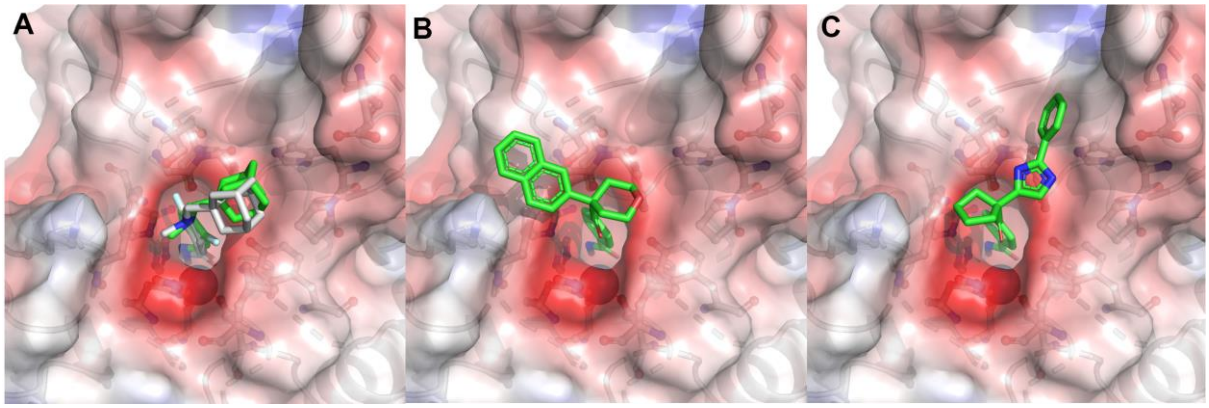

Figure 25. LcHDAC6-D2 protein shown as white ribbon, binding site residues depicted as white ball and sticks with electrostatic surface displayed. Gold docked ligands Bavarostat (a), JT86B (b) and JT19018-4 (c) shown as green sticks. Crystal structure of Bavarostat shown as white sticks (a).

The docking experiments in to lcHDAC6-D2 were then expanded to include commercial inhibitors shown in Figure 23. Glide docking was performed on each of the inhibitors with a metal ion binding constraint applied to the Zn atom and at least one H-bond constraint to either H619 or Y790 was required. The initial poses were then further optimized by performing a Prime MMGBSA calculation that can help to identify more native like poses. Interest in HDAC6 as a medicinal target has increased in recent years and there more than 50 HDAC6 crystal structures have been released. We compare selected docked inhibitor poses with HDAC6 crystal structures with similar inhibitors, Figure 26.

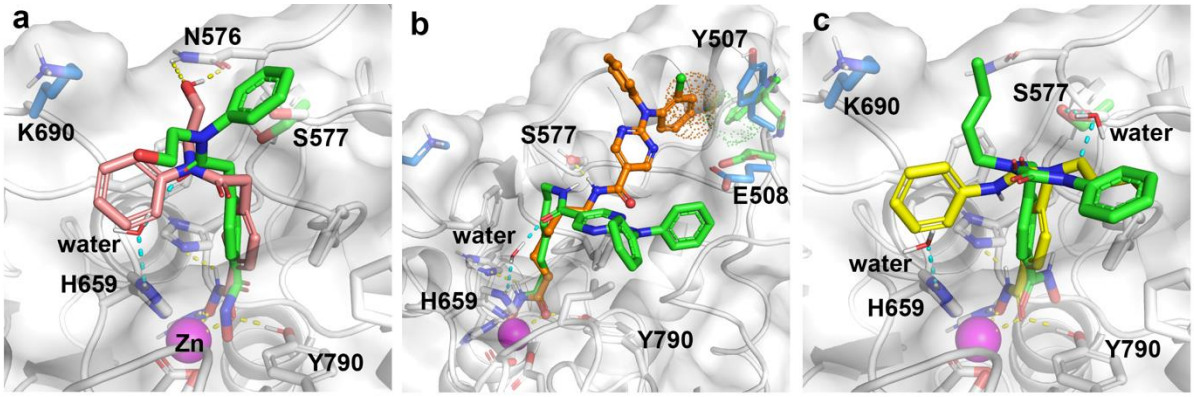

Figure 26. LcHDAC6-D2 protein shown as white ribbon and surface with binding site residue sidechains depicted as white sticks with non-human identical residues high-lighted as light blue sticks. H-bonds from docked structures indicated as dotted yellow lines. Zebra fish drHDAC6-D2 derived crystal structure inhibitors shown as green sticks with bridging crystal waters shown as thin sticks with crystal H-bonds as cyan dotted lines. Docked poses shown as colored sticks. a) HPOB (pink), crystal HPOB (green); b) Citorinostat ACY-241 (orange), crystal analog Ricolinostat ACY-1215 (green); c) Nexturastat A (yellow), crystal Nexturastat A (green).

The commercial inhibitors were successfully docked into the lcHDAC6-D2 model with their final poses indicating they had the potential to be moderate to potent binders. Inhibitors HPOB, BRD73954, Nexturastat A and pyrimidine analog ACY-738 all docked in a bidentate fashion. A comparison of the docked poses of HPOB (Figure 26, panel a) and Nexturastat A (Figure 26, panel c) with corresponding HDAC6 crystal structures reveals different modes of binding. Docked HPOB hydroxamate binds Zn^{2+} in a bidentate fashion. Whereas, in the zebrafish crystal structure of drHDAC6-D2 (5EF7.pdb), HPOB binds Zn^{2+} in a monodentate fashion via the hydroxamate hydroxyl group (Figure 26 panel a). A second water molecule binds the Zn^{2+} ion at the free coordination site. The capping region of HPOB docked the ethoxy group H-bonded to N576 in a donor acceptor arrangement; with the phenyl group sitting in a small pocket above H659. In the crystal structure of bound HPOB a water molecule occupies this small pocket and excludes the crystal phenyl group from this pocket, (Figure 26 panel a). The capping group of the crystal HPOB adopts a completely different pose that is driven by a H-bonded water bridge from the amide carbonyl group of the cap region of HPOB to H659. The capping phenyl group sits above F629 and the free ethoxy group points away from the active site (Figure 26 panel a).

Docking of Citorinostat ACY-241 (Figure 26, panel b) was compared to the crystal structure of a close analog Ricolinostat ACY-1215 bound to drHDAC6-D2 (5WGL.pdb). The hydroxamate groups of both inhibitors bind Zn^{2+} in a bidentate fashion with their alkyl chain linker groups extending through the tunnel region between F629 and F688. However, the capping diphenylamine pyrimidine groups adopted different orientations. The docked conformation of Citorinostat ACY-241 adopts a pose that allows a H-bond to be made from the amide NH to S577. This results in the diphenylamine pyrimidine group being projected between loop 1 and loop 2 of the homology model where Y507 is rotated out creating more room to accommodate the bulky group. In the crystal structure of drHDAC6 Y507 is a tryptophan residue and it is in an inward facing orientation that constricts the binding pocket. This constriction would not favour the binding of the bulky head group of Citorinostat ACY-241 as demonstrated by the overlapping dotted spheres of the clashing atoms between docked pose of Citorinostat ACY-241 and the crystal tryptophan residue, Y507 corresponding green sticks (Figure 26, panel b). Ricolinostat ACY-1215 capping group projects the diphenylamine pyrimidine group over the equivalent loop 1 residue P512 and loop4 residues P756 and L757. This is stabilized by a H-bonding water bridge between the linking amide carbonyl oxygen and H659 (shown Figure 26, panel b). It is interesting to note that the position of crystalized Ricolinostat ACY-1215 places the capping group very close to E508 (Figure 26, panel b). E508 is larger than the corresponding human and zebrafish equivalent aspartate residue and may indicate there is less space for the Citorinostat ACY-241 head group in lcHDAC6-D2.

Nexturastat A also docks in a conformation (Figure 26, panel c) that is significantly different to that observed in a zebrafish drHDAC6-D2 crystal structure (5G0I.pdb). In the crystal structure the hydroxamate group of Nexturastat A binds the Zn^{2+} ion in a monodentate fashion via the carbonyl oxygen. A free water molecule binds the second free Zn^{2+} coordination site. The phenyl linker group of Nexturastat A docks in the binding site tunnel between residues F629 and F688 as does the crystal form. However, the urea linked butyl and benzyl capping groups adopt different orientations. In the docked form the benzyl cap group sits in a small pocket above H659 and the butyl group sits above F629. In the crystal orientation the benzyl group sits above the equivalent of P512 and not H659 as there is a crystal water H-bonded to the crystal equivalent of H659. The butyl group projecting away from the active site in the crystal structure. Neither the crystal or docked forms of Nexturastat A interact with the conserved S577 residue (Figure 26, panel c).

It is clear from examining the docked modelling and crystal structure poses of the inhibitors that solvation by water plays a critical role in stabilizing protein-inhibitor complexes. Docking methods often include the removal of ligand and solvent molecules from the binding site to focus the ligand docking on interactions to protein only. However, this process of exclusion of water from the binding site may lead to misleading and incorrectly docked conformations. Future docking experiments should examine available crystal structures for conserved water molecules and might potentially model these during experiments to improve ligand poses, although this presents many challenges using existing modelling software packages that do not predict flexible protein structures well.

6.4 Sheep experiment

6.4.1 Observations at 24 hours

Each of the sheep assay sites was examined at the 24 hour time point (Table 4). It was noted that the larvae had moved from the piece of paper that had been used to deposit them initially on the sheep, except at one control site, as described more fully below. Larvae at all other control sites appeared active at the skin surface of the sheep. Larvae on many of the sites treated with the higher concentrations of two of the experimental drugs had moved from the initial paper disc, and then had died, and the carcases were visible on the lower surface of the absorbent cloth. The larvae treated with the lower concentrations of these two compounds were still active. Larvae for the third experimental compound appeared to be active at all concentrations tested. Larvae at the highest concentration of cyromazine (ProGuard) were dead, while those at lower concentrations were still active.

It was noted that the larvae had all moved from the underside of the paper disc except in the control site of sheep 8740. The larvae at this site were still on the disc and were dead (Table 4). It is likely that the larvae had 'drowned' here due to excessive moisture being present under the disc at this site. The source of the moisture could have been the water contained within the disc itself when placed onto the sheep, water seeping from the absorbent cloth above, or serum exudate seeping from the skin due to the irritation of the skin with a razor before the larvae were placed onto the site. The larvae appear to have died in this moisture at the site as they have not moved from the disc. The larvae in all other sites, even those with high drug levels that resulted in subsequent death of the larvae,

had moved from the paper disc at the 24 hour time point. Given the abnormal nature of the outcome at this site, with death of larvae in a manner not seen at any other site, the data from this site (zero live larvae recovered) was not used for subsequent calculations of mean larval recovery and mean larval weight from control sites.

6.4.2 Effects of drug treatments on larvae at 48 hours

There was some variation in the numbers of larvae recovered from control sites, and their mean weight (left hand side columns of Figure 27A and 28B, Table 4). The mean (± SE) number of larvae recovered from the control sites (n=5) was 131 ± 23. The mean weight per larva was 3.36 ± 0.87 mg.

The numbers of larvae recovered from drug-treated sites, and their mean weight, are shown in Figure 27A and 28B, respectively. The larval recoveries and weights as a percentage of the means of control sites are shown in 28C and 28D, respectively.

Numbers of larvae in cyromazine (ProGuard)-treated sites decreased from 150 to almost zero (110 % of controls to 0%) as the drug level increased from 0.01 to 0. 1 mg (Log -2 to -1). The BR67c and JT86 treatments showed a similar decrease from control levels to zero as the drug level increased from 0.05 to 0.5 mg (Log -1.3 to -0.3). Therefore, the range of drug levels over which the larval recovery decreased from control levels to zero was about 5-fold higher for the two HDAC inhibitors compared to cyromazine.

There were significant numbers of larvae found at some of the sites treated with BR67c at 5 mg (104 larvae) and at one of the two sites treated with 5 mg of JT86 (43 larvae). However, these larvae were much smaller than controls (26 % of the control weight for BR67c, and 12 % of the control weight for JT86). It is unlikely that these small larvae would have continued to develop to pupation if they had remained at the site in the presence of the drug.

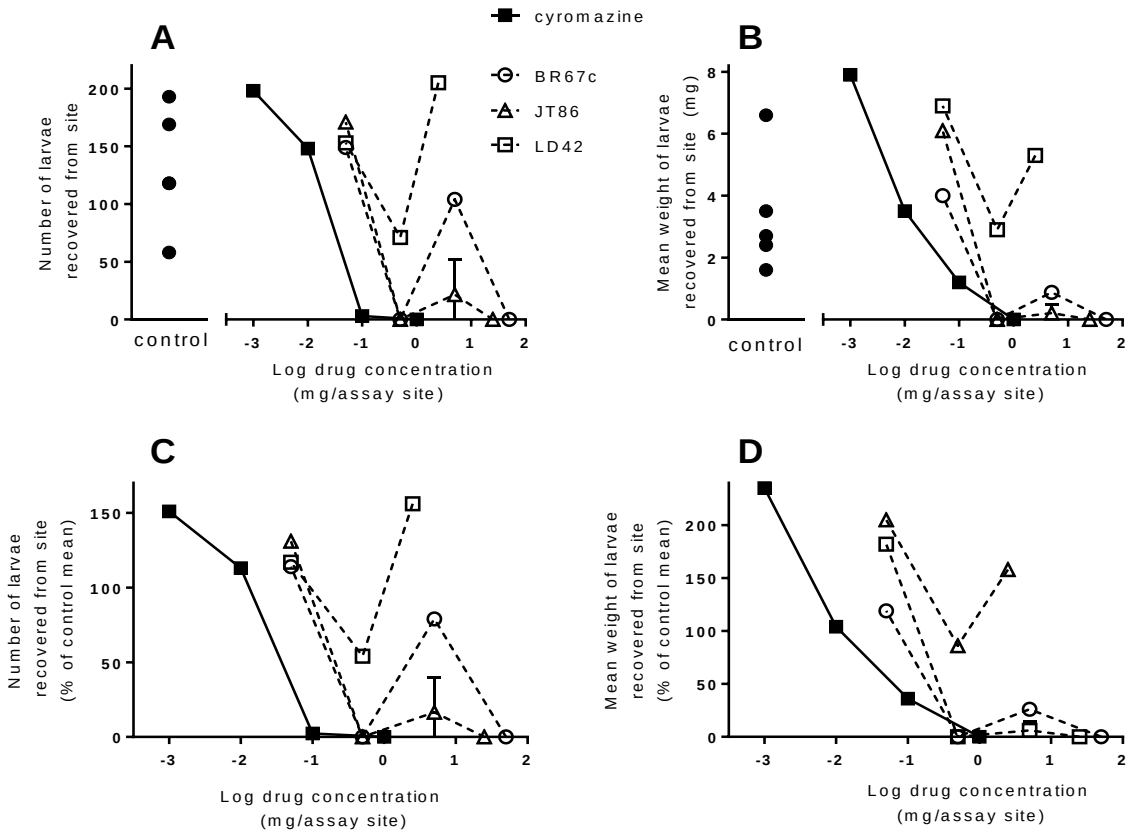

Figure 27: effects of HDAC inhibitors and cyromazine on development of blowfly larvae on sheep:
A: numbers of larvae recovered from drug-treated and control sites
B: mean weight of larvae recovered from drug-treated and control sites
C: numbers of larvae recovered from drug-treated sites as percentage of mean numbers across control sites (n=5)
D: mean weight of larvae recovered from drug-treated sites expressed as percentage of mean numbers across control sites (n=5)

Table 4. Effect of drug treatments on the development of blowfly larvae at infection sites on sheep.

Treatment	Drug level (mg)	Sheep	Comments at 24 hrs	Number of live larvae recovered at 48 hrs	Mean weight per larva (mg)
Control	-	8763	Active, 2.5 mm	169	2.7
	-	8810	As above	118	1.6
	-	8831	As above	58	3.5
	-	8740	Dead on paper disc	0	-
	-	8880	Active, 3-4 mm	193	6.6
	-	8887	Active, 2.5 mm	118	2.4
BR67c	50	8763	Many dead on absorbent cloth	0	-
	50	8887	As above	0	-
	5	8763	Active, 1-1.5 mm	104	0.88
	0.5	8763	Many dead on absorbent cloth	0	-
	0.05	8880	Active, 2.5 mm	149	4.0
JT86	25	8810	Many dead on absorbent cloth	0	-
	5	8810	Active, 1 mm	43	0.41
	5	8887	None visible	0	-
	0.5	8810	None visible	0	-
	0.5	8887	None visible	0	-
	0.05	8880	Active, 3 mm	171	6.1
LD42	2.5	8831	Active, 2.5 mm	205	5.3
	0.5	8831	Active, 1.5 mm	71	2.9
	0.05	8831	Active, 2.5 – 3 mm	153	6.9
ProGuard	1	8740	Many dead on absorbent cloth	0	-
	0.1	8740	Active, 1 mm	3	1.2
	0.01	8740	Active, 2.5 mm	148	3.5
	0.001	8880	Active, 3-4 mm	198	7.9

The data therefore indicates that BR67c and JT86 were able to inhibit larval growth after application to sites on sheep skin (in the presence of short wool). The two compounds prevented larval growth completely at the three sites treated with 0.5 mg of the compounds, representing an approximately 5-fold higher level of the drugs than the level of cyromazine required in order to also completely inhibit larval growth.

Numbers of larvae recovered from sites treated with LD42 remained high as the highest level tested for this compound (2.5 mg) (Figure 27, Table 4). The mean weight of the larvae recovered from this site was greater than the mean control weight. The upper end of the range of drug levels that could be tested for this compound was limited by its lower solubility in ethanol compared to the other two HDAC inhibitor compounds, however, it is clear from Figure 28 that this compound was much less effective against the larvae than BR67c and JT98.

This experiment has demonstrated that HDAC inhibitors applied to sheep skin (in the presence of short wool) are able to prevent the development of blowfly larvae at experimental infection sites. The level of potency is approximately 5-fold lower than that shown by the commercial insecticide cyromazine. The commercial insecticide provides protection against flystrike for an extended period as it remains at sufficiently high levels to prevent larval growth for at least 11 weeks (ProGuard Sheep Blowfly Treatment Product Label). The stability of HDAC inhibitors within the sheep fleece, and hence their ability to provide prolonged control of blowfly strike, remains to be determined.

The experiment has also provided evidence that this method of measuring larva growth at sites on sheep, that was originally developed as a means to assess the immune status of individual sheep (Eisemann et al. 1989), is also useful for investigating the ability of insecticidal agents to prevent blowfly larvae from establishing infections on sheep.

7. Discussion

Control of the sheep blowfly relies largely on the use of chemical insecticides applied as preventative treatments to protect against flystrike. However, recent reports of resistance to the most commonly-used chemicals has highlighted the need for alternative drugs for flystrike control. The present project aimed to explore one avenue of this drug development process by examining the potential for blowfly control based on the use of inhibitors of a specific target in the blowfly not previously examined as an insecticidal drug target.

The project was a collaboration between Professor David Fairlie, from the University of Queensland, and Dr Andrew Kotze, from CSIRO. In a previous AWI-funded project, we showed that inhibitors of a group of enzymes known as histone deacetylases (HDACs) were lethal at high doses to the Australian sheep blowfly. The growth of blowfly larvae exposed to inhibitors of these enzymes was severely inhibited, and the larvae died soon afterwards. HDACs are enzymes that are essential for the regulation of gene transcription in cells. The blocking of their action by drugs results in cell death. In recent years there has been a great deal of interest in developing inhibitors of these enzymes in humans as possible treatments for cancers and inflammatory diseases. Several HDAC inhibitors are currently in clinical use as chemotherapy treatments for humans. They have also been studied extensively over recent years for their potential in chemotherapy for parasitic diseases of humans, including malaria, toxoplasmosis, trypanosomiasis, schistosomiasis and leishmaniasis, especially through a European Framework project in which Professor Fairlie was a partner.

The present project aimed to identify HDAC inhibitors for use as insecticidal compounds for the control of the sheep blowfly. Experimental HDAC inhibitors were rationally designed using homology models of blowfly HDAC structures, chemically synthesised, and their ability to inhibit the development of, and then kill, blowfly larvae was measured using *in vitro* assays. An important aspect of compound design was to ensure that the compounds were of a relatively simple structure that would be amenable to low-cost mass-production, as would be desirable for any commercial insecticide.

We worked with the Protein Expression Facility (PEF) at the University of Queensland to produce recombinant versions of two blowfly HDAC enzymes (*Lc*HDAC1 and *Lc*HDAC6), and then measured the ability of the experimental compounds to inhibit their action in *in vitro* assays. The results of blowfly and enzyme assays with experimental drugs were then used to design a new batch of compounds, based on the structural features that had been associated with a greater ability to kill the blowfly larvae and inhibit the recombinant enzymes. This process continued over a number of cycles of compound design and synthesis, followed by potency testing. We also performed a comprehensive homology modelling study to generate likely structures of the blowfly HDAC enzymes. This then allowed us to model the fit of experimental drugs into the HDAC enzymes, and hence to increase our understanding of what structural features of a drug would likely allow it to best inhibit the enzymes, and hence show greater activity in killing blowfly larvae. The homology modelling also allowed us to study differences that exist between the structures of the enzymes in blowflies and mammals, with a view to exploring the potential for insect-specific inhibitors. Finally, to begin to translate our study from the lab to the field, we conducted a small scale larval-implant trial on sheep using several of our experimental compounds. We examined the ability of blowfly larvae to establish strikes at experimental sites on sheep that had been treated with the compounds.

We synthesised and examined the properties of ten batches of experimental compounds over the course of the study. The most potent compounds had very significant levels of activity against blowfly larvae and against the two blowfly HDAC enzymes. Without any optimisation for blowfly absorption, the best of the compounds was within 4-fold as toxic to blowfly larvae as the commercial blowfly control chemical cyromazine (the active in Vetrazin) in our *in vitro* assays. Importantly, the most potent compounds showed an ability to inhibit the early larval life stages of the blowfly, with complete inhibition of larval growth within the first 24 hours at the highest concentrations tested. This speed of action of the compounds is an important aspect for their potential as insecticides as it is vital for a blowfly control chemical to prevent the larvae developing to a stage that can start to cause significant damage to the sheep. This aspect of their action was also demonstrated in our sheep experiment with the compounds, as described below. Due to the lack of correlations between structure-activity relationships for human and blowfly HDAC enzyme inhibitory potencies and the blowfly larval growth assays (for example, as shown in Figure 11B), we were unable to rationally increase drug potency further. It remains possible that further structural modifications, other than those

assessed to date, to our most potent compounds, may enhance potency. There are clearly still unknown factors that need to be discovered to understand the specific requirements for drug uptake, transport and killing of blowfly larvae under the experimental conditions used. However, despite this, the identification of several compounds with activities against sheep blowfly larvae comparable to a widely-used commercial insecticide indicates the potential for such compounds as blowfly insecticides.

Most of the compounds that potently inhibited blowfly larvae and/or blowfly enzymes were also inhibitors of mammalian HDAC enzymes. The mammalian- versus insect-specificity aspect of HDAC inhibitor compounds is an important issue impacting on the use of these compounds for the control of blowflies on sheep. The homology modelling component of the project addressed this issue by comparing mammalian and blowfly HDACs. We constructed *in-silico* homology models for each of the five blowfly HDAC proteins *Lc*HDAC1, 3, 4, 6 and 11, as identified in its genome. The various blowfly HDACs had between 44 -78% sequence identity with their respective human HDACs (1, 3, 4, 6, 11). We analysed the amino acid differences between blowfly lcHDAC1, 3, 4, and 6 and corresponding human HDACs within 8 Å of the Zn^{2+} atom in the binding site. We found the binding sites of *Lc*HDAC1, 3 and 4 were very similar to human binding sites, with few differences. Hence, the design of new class I selective *Lc*HDAC inhibitors will be challenging. On the other hand, for *Lc*HDAC6, which has two distinct binding sites, we found that each site had significant sequence differences between the human and blowfly sites. We performed molecular docking studies on over 100 potential inhibitors from both commercial and new *in-silico* designed inhibitors. Compounds were docked into models of *Lc*HDAC1 and *Lc*HDAC6 to assess their potential binding modes. This confirmed the difficulty of designing class I blowfly-specific inhibitors. However, for the Class II HDACs 4 and 6, the docking studies confirmed the presence of a number of differences near the binding site of the human and blowfly enzymes. These differences in amino acid residue size, charge and polarity may allow the design of new inhibitors that may prove to be more potent and selective towards individual blowfly HDACs.

Finally, we conducted a sheep trial with three experimental compounds, chosen on the basis of potency, low metabolic degradation by liver microsomes, presence of structurally-distinct features, and low synthetic cost. The compounds were applied to separate experimental sites on sheep, freshly-hatched blowfly larvae were added, and the sites monitored for 48 hours. Any live larvae were then recovered, counted and weighed. We applied cyromazine to some sites as a commercial insecticide treatment to compare to our experimental compounds. Two of the three compounds killed all the larvae at the experimental sites. The level of drug required to kill all larvae was approximately 5-fold higher than the levels of cyromazine required to achieve the same outcome. This indicates that the experimental compounds were able to prevent blowfly larval growth at a concentration comparable to that for the commercial product cyromazine. However, importantly, our experiment only provided a single point in time for examining the effect of the drug. The commercial insecticide provides protection against flystrike for an extended period as it remains at sufficiently high levels to prevent larval growth for at least 11 weeks (ProGuard Sheep Blowfly Treatment Product Label). The stability of HDAC inhibitors within the sheep fleece, and hence their ability to provide prolonged control of blowfly strike, remains to be determined, and has not in any way been optimised at this stage.

The project did not identify any blowfly-specific inhibitors. However, the homology modelling work showed that a focus on the Class II enzymes (for example, LcHDAC6) offers potential for the discovery of such insect-specific inhibitors in the future. It is also clear that complete insect-specificity may not be required for blowfly control as the potency of the experimental compounds identified here means that they can likely be used at levels safe for topical application to mammals, as required for blowfly control. Many safety and tolerability analyses for HDAC inhibitors have been performed in rodents and humans (Shah, 2019) The FDA-approved drugs Vorinostat (SAHA), Romidepsin (FK228; Istodax®), Belinostat (PXD101; Beleodaq®) and Panobinostat (LBH-589; Farydak®) are HDAC inhibitors approved for human use in treating cancer (mainly lymphomas). These compounds are broad spectrum epigenetic modulators that inhibit all or most of the eleven zinc-containing HDAC enzymes and affect up to 10% of the human genome through downstream actions. These particular HDAC inhibitors, which inhibit all 11 known human HDAC enzymes with no specificity, are associated with a range of adverse effects, notably myelosuppression, diarrhoea and various cardiac effects, although most of these are only serious/severe at the highest doses used i.p. or p.o. Up to 100 mg/kg single dose has been given i.p. or p.o. in preclinical animal studies with efficacy and a degree of safety. Mice can be treated safely by oral gavage with 10-50 mg/kg HDAC inhibitor once daily (q.d.) or 10-25 mg/kg twice daily (b.i.d.) for 1 day to 16 weeks. In the case of rodent studies of inflammatory disorders, there is also evidence that much lower daily doses (1mg/kg p.o.) of HDAC inhibitors are sometime more efficacious than these high doses. For topical delivery, the upper doses indicated above are quite safe in mammals. The optimal

compounds chosen for the sheep experiment in this study had high liver microsome stabilities, which is usually important for compounds that are administered systemically (p.o., i.v., i.p.) into animals. For topical application to sheep, the compound is layered on the outer skin, where it is much less exposed to P450 metabolising enzymes. Finally, there is the issue of cytotoxicity. All of the HDAC inhibitors in this report have some degree of cytotoxicity to human skin cells at micro- to milli-molar concentrations. However, while they do show some cytotoxicity, it is an order of magnitude less than the HDAC drugs currently approved for systemic human use.

8. Impact on Wool Industry – now & in 5 years' time

The project represents the first stage of a process in drug development that can take many years. It would be at least 5 years before any insecticide based on inhibition of HDAC enzymes could be delivered to the market, perhaps longer. In the meantime, the wool industry is able to utilise the currently available insecticides, with the knowledge however that resistance to the most widely-used product (CLiK) is emerging. If resistance to this chemical becomes more wide-spread, and resistance also emerges to the currently-used ivermectin- and imidacloprid-based products, the availability of new insecticides will become more important and their rapid development more urgent. It is therefore important that new classes of insecticides, such as the type explored in the present project, are in the development pipeline to provide these future chemical control options.

9. Conclusions and Recommendations

This project has shown that HDAC inhibitors are potent inhibitors of blowfly larval development *in vitro*, and has identified new potent compounds of different structure and chemical compositions to existing insecticides used in the sheep industry. We have shown that the ability to inhibit blowfly larvae *in vitro* also translates to an ability to prevent the development of larvae at experimental implant sites on sheep. Specificity for blowflies over other insects, mammals and humans has not been investigated but we note that HDAC inhibitors can be delivered safely to humans by systemic administration, so topical application to mammals (sheep) is expected to be safe for both sheep and humans who consume them in the diet. Additionally, the homology modelling component of the project has indicated that blowfly-specificity may be attainable by the targeting of the Class II HDAC enzymes in the blowfly. Further development of the outcomes of the present study to develop HDAC inhibitors as insecticides for blowfly control will require the project team engaging with animal health companies.

<u>Recommendations:</u>

- the project team seeks to engage with animal health companies for further work on developing HDAC inhibitors as insecticides for blowfly control.

- more broadly, the project team seeks to engage with animal health companies in order to develop insecticides for blowfly control beyond just the use of HDAC inhibitors, with emphasis on the drug design, chemical synthesis, and parasitology techniques demonstrated in the present project.

10. Bibliography

Alves Avelar LA, Held J, Engel JA, Sureechatchaiyan P, Hansen FK, Hamacher A, Kassack MU, Mordmüller B, Andrews KT, Kurz T. 2017. Design and Synthesis of Novel Anti-Plasmodial Histone Deacetylase Inhibitors Containing an Alkoxyamide Connecting Unit. Arch Pharm (Weinheim). 350: 3-4.

Andrews, K.T., Haque, A., Jones, M.K. 2012. HDAC inhibitors in parasitic diseases. Immunol. Cell Biol. 90, 66-77.

Anstead, C. A., P. K. Korhonen, N. D. Young, R. S. Hall, A. R. Jex, S. C. Murali, D. S. T. Hughes, S. F. Lee, T. Perry, A. J. Stroehlein, B. R. E. Ansell, B. Breugelmans, A. Hofmann, J. Qu, S. Dugan, S. L. Lee, H. Chao, H. Dinh, Y. Han, H. V. Doddapaneni, K. C. Worley, D. M. Muzny, P. Ioannidis, R. M. Waterhouse, E. M. Zdobnov, P. J. James, N. H. Bagnall, A. C. Kotze, R. A. Gibbs, S. Richards, P. Batterham and R. B. Gasser. 2015 . Lucilia cuprina genome unlocks parasitic fly biology to underpin future interventions. Nature Communications 6: 7344.

Bagnall NH, Hines BM, Lucke AJ, Gupta PK, Reid RC, Fairlie DP, Kotze AC. 2017. Insecticidal activities of histone deacetylase inhibitors against a Dipteran parasite of sheep, Lucilia cuprina. Int J Parasitol Drugs Drug Resist. 7: 51-60.

Bass C, Denholm I, Williamson MS, Nauen R. 2015. The global status of insect resistance to neonicotinoid insecticides. Pestic Biochem Physiol. 121:78-87

Bayer T, Chakrabarti A, Lancelot J, Shaik TB, Hausmann K, Melesina J, Schmidtkunz K, Marek M, Erdmann F, Schmidt M, Robaa D, Romier C, Pierce RJ, Jung M, Sippl W. 2018. Synthesis, Crystallization Studies, and in vitro Characterization of Cinnamic Acid Derivatives as SmHDAC8 Inhibitors for the Treatment of Schistosomiasis. ChemMedChem. 13:1517-1529

Bouchut A, Rotili D, Pierrot C, Valente S, Lafitte S, Schultz J, Hoglund U, Mazzone R, Lucidi A, Fabrizi G, Pechalrieu D, Arimondo PB, Skinner-Adams TS, Chua MJ, Andrews KT, Mai A, Khalife J. 2019. Identification of novel quinazoline derivatives as potent antiplasmodial agents. Eur J Med Chem. 161:277-291

Chua MJ, Arnold MS, Xu W, Lancelot J, Lamotte S, Späth GF, Prina E, Pierce RJ, Fairlie DP, Skinner-Adams TS, Andrews KT. 2017. Effect of clinically approved HDAC inhibitors on Plasmodium, Leishmania and Schistosoma parasite growth. Int J Parasitol Drugs Drug Resist. 7:42-50

Diedrich D, Stenzel K, Hesping E, Antonova-Koch Y, Gebru T, Duffy S, Fisher G, Schöler A, Meister S, Kurz T, Avery VM, Winzeler EA, Held J, Andrews KT, Hansen FK. 2018. One-pot, multi-component synthesis and structure-activity relationships of peptoid-based histone deacetylase (HDAC) inhibitors targeting malaria parasites. Eur J Med Chem. 158:801-813

Dowling, D. P., L. Di Costanzo, H. A. Gennadios and D. W. Christianso. 2008. volution of the arginase fold and functional diversity.Cellular and molecular life sciences : CMLS 65(13): 2039-2055.

Eisemann CH, Johnston LAY, Kerr JD. 1989. New techniques for measuring the growth and survival of larvae of Lucilia cuprina on sheep. Aust. Vet. J. 66, 187-189.

Engel JA, Jones AJ, Avery VM, Sumanadasa SD, Ng SS, Fairlie DP, Skinner-Adams T, Andrews KT. 2015. Profiling the anti-protozoal activity of anti-cancer HDAC inhibitors against Plasmodium and Trypanosoma parasites. Int J Parasitol Drugs Drug Resist. 5:117-126.

Guerrant W, Mwakwari SC, Chen PC, Khan SI, Tekwani BL, Oyelere AK. 2010. A structure-activity relationship study of the antimalarial and antileishmanial activities of nonpeptide macrocyclic histone deacetylase inhibitors. ChemMedChem. 58:1232-5

Guo F, Zhang H, McNair NN, Mead JR, Zhu G. 2018. The Existing Drug Vorinostat as a New Lead Against Cryptosporidiosis by Targeting the Parasite Histone Deacetylases. J Infect Dis. 217:1110-1117

Heimburg T, Chakrabarti A, Lancelot J, Marek M, Melesina J, Hauser AT, Shaik TB, Duclaud S, Robaa D, Erdmann F, Schmidt M, Romier C, Pierce RJ, Jung M, Sippl W. 2016. Structure-Based Design and Synthesis of Novel Inhibitors Targeting HDAC8 from Schistosoma mansoni for the Treatment of Schistosomiasis. J Med Chem. 59:2423-35

Kotze AC, Hines BM, Bagnall NH, Anstead CA, Gupta P, Reid RC, Ruffell AP, Fairlie DP. 2015. Histone deacetylase enzymes as drug targets for the control of the sheep blowfly, Lucilia cuprina. Int J Parasitol Drugs Drug Resist. 5:201-208.

Kotze AC, Prichard RK. 2016. Anthelmintic Resistance in Haemonchus contortus: History, Mechanisms and Diagnosis. Adv Parasitol. 93:397-428

Levot GW. 2012. Cyromazine resistance detected in Australian sheep blowfly. Aust Vet J. 90:433-437.

Levot GW, Langfield BJ, Aiken DJ. 2014. Survival advantage of cyromazine-resistant sheep blowfly larvae on dicyclanil- and cyromazine-treated Merinos. Aust Vet J. 92:421-426

Mackwitz MKW, Hesping E, Antonova-Koch Y, Diedrich D, Gebru T, Skinner-Adams T, Clarke M, Schöler A, Limbach L, Kurz T, Winzeler EA, Held J, Andrews K, Hansen FK. 2019. Structure-Activity and Structure-Toxicity Relationships of Novel Peptoid-Based Histone Deacetylase Inhibitors with Dual-Stage Antiplasmodial Activity. ChemMedChem. In press

Marek M, Kannan S, Hauser AT, Moraes Mourão M, Caby S, Cura V, Stolfa DA, Schmidtkunz K, Lancelot J, Andrade L, Renaud JP, Oliveira G, Sippl W, Jung M, Cavarelli J, Pierce RJ, Romier C. 2013. Structural basis for the inhibition of histone deacetylase 8 (HDAC8), a key epigenetic player in the blood fluke Schistosoma mansoni. PLoS Pathog. 9:e1003645

Marek M, Oliveira G, Pierce RJ, Jung M, Sippl W, Romier C. 2015. Drugging the schistosome zinc-dependent HDACs: current progress and future perspectives. Future Med Chem. 7:783-800.

MLA 2015. Priority list of endemic diseases for the red meat industries. Project code B.AHE.0010, 282pp.

Ontoria JM, Paonessa G, Ponzi S, Ferrigno F, Nizi E, Biancofiore I, Malancona S, Graziani R, Roberts D, Willis P, Bresciani A, Gennari N, Cecchetti O, Monteagudo E, Orsale MV, Veneziano M, Di Marco A, Cellucci A, Laufer R, Altamura S, Summa V, Harper S. 2016. Discovery of a Selective Series of Inhibitors of Plasmodium falciparum HDACs. ACS Med Chem Lett. 7:454-9

Patil V, Guerrant W, Chen PC, Gryder B, Benicewicz DB, Khan SI, Tekwani BL, Oyelere AK. 2010. Antimalarial and antileishmanial activities of histone deacetylase inhibitors with triazole-linked cap group. Bioorg Med Chem. 18:415-25.

Sales N, Suann M, Koeford K. 2020. Dicyclanil resistance in the Australian sheep blowfly, Lucilia cuprina, substantially reduces flystrike protection by dicyclanil and cyromazine based products. Int J Parasit.: Drugs Drug Resist. (in press).

Shah, RR. 2019. Safety and Tolerability of Histone Deacetylase Inhibitors in Oncology, Drug Safety 42, 235–245.

Stenzel K, Chakrabarti A, Melesina J, Hansen FK, Lancelot J, Herkenhöhner S, Lungerich B, Marek M, Romier C, Pierce RJ, Sippl W, Jung M, Kurz T. 2017a. Isophthalic Acid-Based HDAC Inhibitors as Potent Inhibitors of HDAC8 from Schistosoma mansoni. Arch Pharm (Weinheim) 350(8).

Stenzel K, Chua MJ, Duffy S, Antonova-Koch Y, Meister S, Hamacher A, Kassack MU, Winzeler E, Avery VM, Kurz T, Andrews KT, Hansen FK. 2017b. Design and Synthesis of Terephthalic Acid-Based Histone Deacetylase Inhibitors with Dual-Stage Anti-Plasmodium Activity. ChemMedChem. 12:1627-1636

Stolfa DA, Marek M, Lancelot J, Hauser AT, Walter A, Leproult E, Melesina J, Rumpf T, Wurtz JM, Cavarelli J, Sippl W, Pierce RJ, Romier C, Jung M. 2014. Molecular basis for the antiparasitic activity of a mercaptoacetamide derivative that inhibits histone deacetylase 8 (HDAC8) from the human pathogen schistosoma mansoni. J Mol Biol. 426:3442-53

11. Acknowledgements

We thank Neil Bagnall for performing the blowfly HDAC enzyme assays, and the *in vitro* blowfly bioassays, and Tony Vuocolo and Suzie Briscoe for assistance with the sheep experiment.

We also thank senior researchers Drs Robert Reid, Ligong Liu and Jeff Mak for chemistry support, Dr Andrew Lucke for computer modelling, students Ms Jiahui Tng and Mr Lilong Dong for contributing chemistry support, and Dr James Lim and Ms Kai-Chen Wu for conducting additional bioassays.

12. Abbreviations

HDAC = histone deacetylase

*Hs*HDAC1 = human (*Homo sapiens*) HDAC1

IC_{50} = concentration of drug required to inhibit larval weight gain, pupation rate, or enzyme activity to 50 % of the value measured in control assays (in the absence of drug)

LcHDAC1 = *Lucilia cuprina* HDAC1 enzyme

PEF = Protein Expression facility